Effect of Axially Projected Oligothiophene Pendants and Nitro-Functionalized Diimine Ligands on the Lowest Excited State in Cationic Ir(III) bis-Cyclometalates

ARTICLE *in* INORGANIC CHEMISTRY · APRIL 2012

Impact Factor: 4.76 · DOI: 10.1021/ic202573y · Source: PubMed

7 AUTHORS, INCLUDING:

Pere Miró
Jacobs University
46 PUBLICATIONS **649** CITATIONS
SEE PROFILE

Christopher J Cramer
University of Minnesota Twin Cities
531 PUBLICATIONS **23,142** CITATIONS
SEE PROFILE

Kent R Mann
University of Minnesota Twin Cities
178 PUBLICATIONS **7,811** CITATIONS
SEE PROFILE

Effect of Axially Projected Oligothiophene Pendants and Nitro-Functionalized Diimine Ligands on the Lowest Excited State in Cationic Ir(III) bis-Cyclometalates.

Kyle R. Schwartz, Raghu Chitta, Jon N. Bohnsack, Darren J. Ceckanowicz, Pere Miró, Christopher J. Cramer*, Kent R. Mann*.

Department of Chemistry and Supercomputing Institute, University of Minnesota, 207 Pleasant Street SE, Minneapolis, Minnesota 55455

Abstract

The novel terthiophene (3T) oligomer **6** and a series of cationic Ir(III) bis-cyclometalates $[Ir(C^N)_2(N^N)]PF_6$ **9** – **12** were prepared. The synthesis, characterization, electrochemical, and photophysical properties are reported. The cyclometalating ligands (C^N) are 2–phenylpyridinato (ppy) or the 3T oligomer (3T–ppy), asymmetrically capped in the 5 and 5″ positions with the ppy and mesityl groups. The diimine ligands (N^N) are 2,2'–bipyridine (bpy) or 4–NO_2–bipyridine (4–NO_2–bpy). Hybrid metal-organic complexes **11** and **12** bear 3T–pendants ligated through the ppy cap, **10** and **12** contain NO_2 functionalized diimines, whereas **9** contains neither. Structural characterization of **10** by single crystal X-ray diffraction confirms the presence of the NO_2 substituent and pseudo-octahedral coordination geometry about the Ir(III) ion. Cyclic voltammetry highlights the large electron withdrawing effect of the NO_2 substituent, providing an 850 mV shift towards lower potentials for the first diimine centered reduction of **10** and **12**. Strong overlap of the intense $\pi \rightarrow \pi^*$ absorptions of the 3T–pendants with Ir(III) charge transfer bands is evident in complexes of **11** and **12**, precluding the possibility for selective excitation of either chromophore. Photoexcitation (λ_{ex} = 400 nm) of the series affords strong luminescence from the 3T oligomer **6** and the unsubstituted **9**, with ϕ_{em} = 0.11. In stark contrast the NO_2 and 3T functionalized complexes **10** – **12** display near total quenching of luminescence. Computations of the ground and excited state electronic structure using DFT and TD-DFT indicate that both the NO_2 and 3T substituents play an important role in excited state deactivation of complexes **10** – **12**. A substantial electronic contribution of the NO_2 substituent results in stabilization of the diimine based MO and offers an efficient non-radiative decay pathway

for the excited state. Spin-orbit coupling effects of the Ir(III) ion lead to efficient population of the low lying, non-luminescent, triplet states centered on the 3T–pendants.

Introduction

Over the last several decades the properties of electro and photoredox active transition metal species have been extensively investigated. Most notable among this class of molecules are the Ru(II) polypyridyls, the most successful inorganic sensitizers for dye-sensitized solar cell (DSSC) applications.[1] The isostructural Ir(III) cyclometalates, have also found use in a variety of applications ranging from biolabelling agents[2] and oxygen sensors[3] to electron transfer arrays[4], photo-catalytic hydrogen production[5], and light-harvesting materials.[6] Perhaps the true strength of Ir(III) cyclometalates is found as phosphorescent materials in organic light-emitting diodes (OLEDs) [6a, 7] and most recently for the fabrication of electroluminescent devices known as light-emitting electrochemical cells (LECs).[8]

The desirable photophysical properties of Ir(III) cyclometalates, such as high emission quantum yields, favorable excited state lifetimes, photostability, and spectral tuning through ligand modification have been exploited for the fabrication of OLEDs as well LECs.[4d, 7e, 9] LECs utilize ionic luminescent materials in the active layer, bringing charged transition metal species to the forefront. This is to the advantage of the field as the synthetic steps required to yield cationic Ir(III) bis-cyclometalates are relatively straightforward and isomer free compared their neutral tris-cyclometalated congeners.[2a, 4h, 7e, 9e, 9n, 10]

Taking into consideration the many favorable attributes of cationic Ir(III) bis-cyclometalates, their use in devices for light-to-energy or energy-to-light does not come without challenges, such as minimizing concentration based quenching (triplet-triplet annihilation) and enhancing spectral coverage of these phosphorescent materials. These

obstacles have been approached using several strategies. Aggregation can be discouraged and charge transport enhanced by adjusting the amount of phosphorescent dopant found in the supportive hole transporting matrix[11] or by employing a single layer of a sterically encumbered phosphorescent material.[8a, 8g, 8h, 8j, 12] Previous work from others, as well as our own research lab, has been concerned with the synthesis, photophysical and electrochemical properties of various Ru(II) and Os(II) polypyridyls functionalized with oligothiophenes. These studies highlight the importance of organic chromophores in the construction of photoredox active dyads.[13] We expect enhanced spectral coverage to be provided by strongly absorbing oligothiophene chromophores and the possibility of hole transfer after selective hole generation at the metal chromophore, enhancing charge separation. With these considerations in mind we have designed a metal-organic hybrid motif consisting of a cationic Ir(III) bis-cyclometalate possessing axially projected steric bulk in the form of π–conjugated, hole transporting, photoredox active oligothiophene chromophores. The interplay of the metal and organic chromophores in the excited state makes this motif an interesting candidate for light-to-energy or energy-to-light devices. To our knowledge this is the first example of a cationic Ir(III) bis-cyclometalate to utilize axially projected photoredox active pendants in this manner.

Herein we present the synthesis, characterization, and studies of the photophysical and electrochemical properties of a series of cationic Ir(III) bis-cyclometalates of the type $[Ir(C^N)_2(N^N)]PF_6$ (C^N = cyclometalating ligand, N^N = diimine ligand) as shown in Figure 1. Two control complexes ($[Ir(ppy)_2(bpy)]PF_6$ (**9**) and $[Ir(ppy)_2(4–NO_2–bpy)]PF_6$ (**10**)) were synthesized to aid in understanding the photophysical and electrochemical properties of the series. These complexes provide a reference for the systematic

introduction of the functionalized terthiophene (3T) pendants and electron withdrawing NO_2 substituents found in complexes $[Ir(3T–ppy)_2(bpy)]PF_6$ (**11**) and $[Ir(3T–ppy)_2(4–NO_2–bpy)]PF_6$ (**12**) respectively. The 3T–pendants, selected for their well documented spectroscopic and electrochemical properties,[14] were functionalized with *n*–Bu chains and capped with mesityl groups to increase solubility and decrease aggregation. The 3T–pendants were placed *para* to the heteroatom of the pyridyl moiety to maximize axial projection (Figure 1); functionalization at this location has not been well studied for this class of compounds.[6a, 9k, 15] Finally, the NO_2 substituent in complexes **10** and **12** is predicted to lower the energy gap of the MLCT transition, acting as a trap for the lowest triplet excited state. This stabilization should also make reduction of the diimine facile and enhance charge separation.[4h, 7e, 9d, 9f, 9j, 9l, 9p, 16]

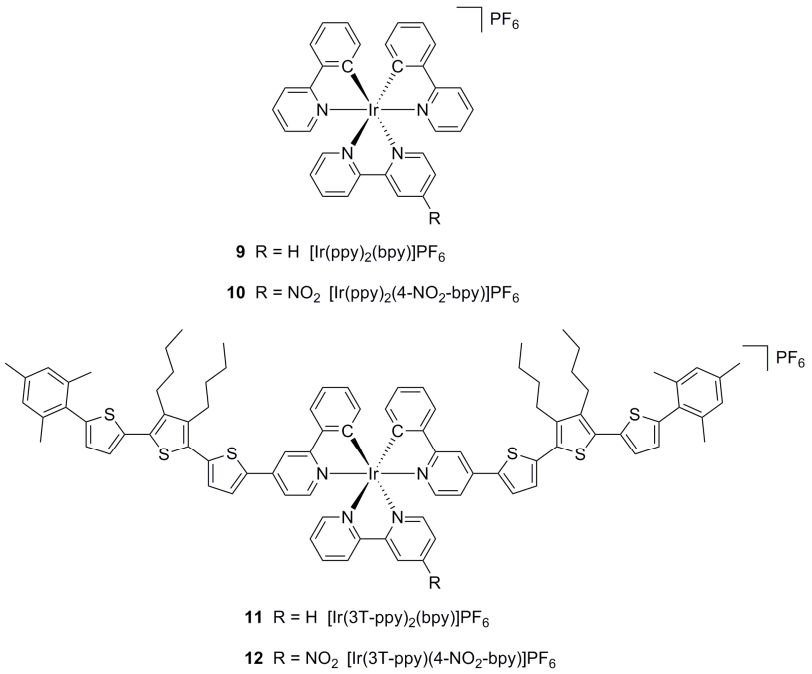

9 R = H $[Ir(ppy)_2(bpy)]PF_6$

10 R = NO_2 $[Ir(ppy)_2(4\text{-}NO_2\text{-}bpy)]PF_6$

11 R = H $[Ir(3T\text{-}ppy)_2(bpy)]PF_6$

12 R = NO_2 $[Ir(3T\text{-}ppy)(4\text{-}NO_2\text{-}bpy)]PF_6$

Figure 1. Molecular structures of cationic Ir(III) bis-cyclometalates. Control complexes **9**, **10**, and 3T–pendant complexes **11**, **12**.

Experimental Section

Safety Note. *CAUTION!* Appropriate safety measures should be followed when using the organolithium and organostannane reagents described here due to their pyrophoric and toxic natures, respectively.

General Considerations. NMR spectra were recorded on a Varian Unity or Varian Inova 300 MHz instrument. High-resolution mass spectrometry was performed on a Bruker BioTOF II mass spectrometer, Hewlett-Packard Series II Model 5890 gas chromatograph/Finnigan MAT 95 mass spectrometer, or Bruker Biflex III MALDI-TOF. All solvents and reagents used for synthetic procedures were purchased from commercially available sources and used without further purification. The following chemicals were used as provided: $IrCl_3 \cdot 3H_2O$ (Johnson Matthey), 2–phenylpyridine (Hppy) (Aldrich), 2,2′–bipyridine (bpy) (TCI Amercia), $NaPF_6$ (Aldrich).

Compounds 2,2′–bipyridine–N–oxide,[17] 4–nitro–2,2′–bipyridine–*N*–oxide,[18] and 3′,4′–dibutyl–2,2′:5′,2″–terthiophene (3′,4′–*n*–Bu–3T)[19] were synthesized according to the reported literature procedures. The cyclometalated Ir(III) dichloro-bridged dimers, $[Ir(ppy)_2(\mu\text{–}Cl)]_2$ (**7**) and $[Ir(3T\text{–}ppy)_2(\mu\text{–}Cl)]_2$ (**8**) were prepared using the method of Watts from $IrCl_3 \cdot 3H_2O$ in a mixture of 2–methoxyethanol and water with slight modification.[20] A series $Ir[(C^N)(N^N)]^+$ (**9** – **12**) complexes was prepared by cleavage of the corresponding dimers with an appropriate diimine ligand and subsequent metathesis to PF_6^- salts as previously described with slight modifications.[2a] Details for all procedural modifications are provided below.

4–Nitro–2,2′–bipyridine (1): Compound **1** was synthesized according to the literature procedure with slight modifications.[21] PCl_3 (16.1 mL, 25.3 g, 0.185 mol) was

added by syringe to a three neck round bottom flask containing 4–nitro–2,2′–bipyridine–*N*–oxide (1.0 g, 4.6 mmol) and the reaction mixture was refluxed (85 °C) under an inert gas atmosphere for 24 h. The reaction mixture was allowed to cool, then poured onto ice and stirred for 30 min. The reaction mixture was brought to a pH of ~11 through the dropwise addition of aq. NaOH, followed by extraction into $CHCl_3$. The organic extract was dried over Na_2SO_4 and evaporated to give **1** as a white solid. Yield: 97%. ^{1}H NMR (300 MHz, CD_2Cl_2): δ 9.13 (dd, 1H, *J* = 2.4, 0.6 Hz), 8.95 (dd, 1H, *J* = 5.4, 0.6 Hz), 8.73 (ddd, 1H, *J* = 4.8, 1.8, 0.9 Hz), 8.48 (ddd, 1H, *J* = 7.8, 1.2, 0.9 Hz), 8.01 (dd, 1H, *J* = 5.1, 2.1 Hz), 7.89 (ddd, 1H, *J* = 7.8, 7.8, 1.8 Hz), 7.42 (ddd, 1H, *J* = 7.5, 4.5, 1.2 Hz).

4–Bromo–2–phenylpyridine (2): Compound **2** was synthesized according to the literature procedures with slight modifications.[22] A solution of 4–bromopyridine (10 g, 0.052 mol) in dry THF (200 mL) was cooled to −78 °C to which a solution of phenylmagnesium chloride (2 M) in THF (65 mL) was added dropwise at −78 °C and allowed to stir for 15 min. Phenylchloroformate (8.0 mL, 10 g, 0.064 mol) in THF (20 mL) was then added dropwise over 10 min at −78 °C after which the reaction mixture was allowed to warm to r.t. The reaction mixture was cooled to 0 °C and quenched with 20% NH_4Cl followed by stirring at 0 °C for 2 h and extraction into diethylether. The combined extracts were washed with H_2O, 20% HCl and H_2O. The organic layer was dried over Na_2SO_4 and evaporated under vacuum to yield a pale yellow material. The residue was dissolved in dry toluene (200 mL) and *o*–chloronil (15.86 g, 0.06451 mol) dissolved in glacial acetic acid (120 mL) was added dropwise, the resultant red solution was stirred at r.t. for 36 h. The solution was made basic using aq. 10% NaOH, filtered through Celite and washed with H_2O. The organic layer was extracted three times using

aq. 10% HCl. The aqueous layers were made basic with NaOH and extracted with CH_2Cl_2. The combined organic layers were dried over Na_2SO_4 and the solvent was removed under vacuum to give the crude compound as a red oil. Purification of the crude compound by column chromatography (silica gel, hexanes:ethylacetate 98:2 – 95:5 v/v) yielded **2** as a pale yellow oil. Yield: 79%. ^{1}H NMR (300 MHz, $CDCl_3$): δ 8.52 (d, 1H, *J* = 5.1 Hz), 7.99–7.96 (m, 2H), 7.91 (d, 1H, *J* = 1.8 Hz), 7.53–7.45 (m, 3H), 7.41 (dd, 1H, *J* = 5.4, 1.8 Hz).

5–Bromo–3′,4′–dibutyl–2,2′:5′,2″–terthiophene (3): Compound **3** was synthesized according to the literature procedure with slight modifications.[23] 3′,4′–*n*–Bu–3T (4.0 g, 0.011 mol), was added to a round bottom flask and pumped/purged with Ar (3 times). DMF (25 mL) was added to the flask and the resulting solution purged for 15 min, then cooled to 0 °C. A solution of *N*–bromosuccinimide (2.0 g, 0.011 mol) in DMF (6 mL) was then added dropwise over 45 min. The reaction mixture was stirred for 3 h at 0 °C, warmed to r.t. and allowed to stir an additional 21 h, followed by the addition of water (20 mL) and CH_2Cl_2 (15 mL). The resulting organic phase was separated and the aqueous phase extracted with CH_2Cl_2 (3 x 15 mL). The combined organic extracts were washed with H_2O (3 x 15 mL) and brine (1 x 20 mL), and then dried over $MgSO_4$. The solvent was removed via rotary evaporation to yield the crude product as a brown-yellow oil. The crude product was purified via column chromatography (silica gel, hexanes) to yield **3** as a yellow oil. Yield: 79%. ^{1}H NMR (300 MHz, CD_2Cl_2): δ 7.35 (dd, 1H, *J* = 5.1 Hz, 1.2 Hz), 7.14 (dd, 1H, *J* = 3.6 Hz, 1.2 Hz), 7.08 (dd, 1H, *J* = 5.1 Hz, 3.6 Hz), 7.04 (d, 1H, *J* = 3.9 Hz), 6.90 (d, 1H, *J* = 3.9 Hz), 2.73 – 2.65 (m, 4H), 1.58 – 1.38 (m, 8H), 0.97 – 0.90 (m, 6H).

5–Mesityl–3′,4′–dibutyl–2,2′:5′,2″–terthiophene (4): **3** (2.5 g, 5.7 mmol), 2,4,6–trimethylphenyl boronic acid (1.12 g, 6.83 mmol), tetrakis(triphenylphosphine)palladium(0) (0.53 g, 0.46 mmol), and K_2CO_3 (2.4 g, 0.017 mol) were added to a round bottom flask and pumped/purged with Ar (3 times). A mixture of dimethoxyethane and H_2O (v/v, 35:11.6 mL) was degassed and added to the flask via cannulation. The reaction mixture was refluxed for 24 h then cooled to r.t., after which H_2O (20 mL) and hexanes (50 mL) were added. The resulting aqueous phase was extracted with hexanes (3 x 75 mL). The combined organic extracts were washed with water (3 x 100 mL), and then dried over Na_2SO_4. The solvent was removed via rotary evaporation to yield the crude product as a brown oily solid. The crude product was purified via column chromatography (alumina, hexanes) to yield **4** as a yellow oil. Yield: 82%. ^{1}H NMR (300 MHz, CD_2Cl_2): δ 7.34 (dd, 1H, J = 5.4 Hz, 1.2 Hz), 7.16 (dd, 1H, J = 3.9 Hz, 1.2 Hz), 7.14 (d, 1H, J = 3.6 Hz), 7.08 (1H, dd, J = 5.4 Hz, 3.6 Hz), 6.95 (s, 2H), 6.76 (d, 1H, J = 3.6 Hz), 2.79 – 2.70 (m, 4H), 2.31 (s, 3H), 2.17 (s, 6H), 1.60 – 1.50 (m, 4H), 1.48 – 1.43 (m, 4H), 0.98 – 0.90 (m, 6H). HRMS (GC-MS EI) $[M\cdot]^+$: calcd for $C_{23}H_{34}S_3$ 478.1823, found 478.1790.

5–((Tributyl)stannyl)–5″–mesityl–3′,4′–dibutyl–2,2′:5′,2″–terthiophene (5): **4** (2.10 g, 4.39 mmol) was added to an oven dried Schlenk flask and pumped/purged with Ar. THF (30 mL) was added and the solution was cooled to −78 °C with a dry ice/isopropanol bath. *n*–butyllithium (2.40 mL, 4.82 mmol) was added dropwise over 45 min, and the solution was stirred for an additional 30 min at −78 °C, followed by the addition of tributyltin chloride (1.50 mL, 5.27 mmol). The solution was warmed to r.t. and stirred for 1 h, followed by the addition of H_2O (10 mL) and hexanes (10 mL). The

resulting organic phase was separated and the aqueous phase extracted with hexanes (3 x 20 mL). The combined organic extracts were washed with H_2O (2 x 50 mL) and a saturated solution of aq. $NaHCO_3$ (2 x 50 mL), and then dried over $MgSO_4$. The solvent was removed via rotary evaporation to yield **5** as a yellow-brown oil Yield: 82%. The material as isolated was considered a reaction intermediate that was pure enough for use without purification. ^{1}H NMR (300 MHz, CD_2Cl_2): δ 7.27 (d, 1H, *J* = 3.3 Hz), 7.13 (d, 2H, *J* = 3.6 Hz), 6.95 (s, 2H), 6.75 (d, 1H, *J* = 3.6 Hz) 2.78 – 2.71 (m, 4H), 2.31 (s, 3H), 2.17 (s, 6H), 1.63 – 1.30 (m, 20H), 1.17 – 1.11 (m, 6H), 1.0 – 0.90 (m, 15H).

4–(3′,4′–Dibutyl–5′′–mesityl–2,2′:5′,2′′–terthiophen–5–yl)–2–phenylpyridine (H3T–ppy, 6): **5** (1.08 g, 1.40 mmol), **2** (0.30 g, 1.3 mmol), and tetrakis(triphenylphosphine)palladium(0) (0.08 g, 0.07 mmol) were added to an oven dried Schlenk flask and pumped/purged with Ar. DMF (25 mL) was degassed and added to the flask via cannulation and the reaction mixture was heated to 100 °C for 48 h. The solution was cooled to r.t., transferred to a separatory funnel followed by the addition of H_2O (50 mL) and ethyl acetate (50 mL). The resulting organic phase was separated and the aqueous phase extracted with ethyl acetate (4 x 50 mL). The combined organic extracts were washed with water (4 x 100 mL) and a saturated solution of aq. $NaHCO_3$ (1 x 75 mL), and then dried over Na_2SO_4. The solvent was removed via rotary evaporation to yield the crude product as a red-brown oil. The crude material was purified via column chromatography (silica gel, CH_2Cl_2:hexanes 75:25 to 100 CH_2Cl_2) to yield **6** as a thick red oil. Yield: 78%. ^{1}H NMR (300 MHz, CD_2Cl_2) δ 8.66 (dd, 1H, *J* = 5.4 Hz, 0.6 Hz), 8.07 (ddd, 1H, *J* = 5.7 Hz, 3.0 Hz, 1.5 Hz), 7.94 (dd, 1H, *J* = 1.8 Hz, 0.9 Hz), 7.59 (d, 1H, *J* = 3.9 Hz), 7.48 (m, 5H), 7.22 (d, 1H, *J* = 3.9 Hz), 7.17 (d, 1H, *J* = 3.6 Hz), 6.95

(s, 2H) 6.77 (d, 1H, *J* = 3.6 Hz), 2.82 – 2.74 (m, 4H), 2.31 (s, 3H), 2.17 (s, 6H), 1.61 – 1.42 (m, 8H), 1.00 – 0.94 (m, 6H). HRMS (ESI-TOF) $[M + H]^+$: calcd for $C_{40}H_{42}NS_3$ 632.2474, found 632.2464.

$[Ir(3T–ppy)_2Cl]_2$ (8): A solution of **6** (0.30 g, 0.48 mmol) in 2–methoxyethanol (15 mL) was added to a flask containing $IrCl_3 \cdot 3H_2O$ (0.08 g, 0.2 mmol) and H_2O (5 mL). The reaction mixture was allowed to reflux under an inert gas atmosphere for 24 h. After cooling to r.t. a red precipitate was collected by filtration. The reaction solid was dried by suction and dissolved off the frit with CH_2Cl_2 then concentrated by rotary evaporation. Precipitation was induced by addition of diethyl ether under a stream of N_2. The solid was filtered and washed with diethyl ether. Compound **8** was obtained as a brick red solid in a crude yield of 70% and used without further purification. ^{1}H NMR (300 MHz, CD_2Cl_2): δ 9.28 (d, 4H, *J* = 6.3 Hz), 8.15 (s, 4H), 7.70 (d, 4H, *J* = 7.5 Hz), 7.59 (d, 4H, *J* = 3.9 Hz), 7.25 (d, 4H, *J* = 3.9 Hz), 7.14 (d, 4H, *J* = 3.6 Hz), 7.02 (dd, 4H, *J* = 6.3, 1.8 Hz), 6.94 (s, 8H), 6.89 (t, 4H, *J* = 7.5 Hz), 6.73 (d, 4H, *J* = 3.6 Hz) 6.68 (t, 4H, *J* = 7.5 Hz), 6.12 (d, 4H, *J* = 7.8 Hz), 2.71 (q, 16H, *J* = 7.2 Hz), 2.32 (s, 12H), 2.16 (s, 24H), 1.46 (m, 32H), 0.989 (t, 12H, *J* = 6.6 Hz), 0.910 (t, 12H, *J* = 7.2 Hz). MS (MALDI-TOF) $[M – C_{80}H_{80}Cl_2IrN_2S_6]^+$: calcd for $C_{80}H_{80}IrN_2S_6$ 1453.427, found 1453.427.

$[Ir(ppy)_2(bpy)]PF_6$ (9): $[Ir(ppy)_2Cl]_2$ (0.17 g, 0.16 mmol), and 2,2′–bipyridine (0.053 g, 0.34 mmol) were refluxed under an inert gas atmosphere in a 1:1 mixture of CH_2Cl_2:CH_3OH for 6 h. The reaction mixture was allowed to cool to r.t. and then concentrated by rotary evaporation. Diethyl ether was added to induce precipitation followed by filtration and washing with diethyl ether. Solid was then dissolved in CH_3OH. Addition of $NaPF_6$ (0.31 g) to the solution while stirring resulted in a bright

yellow precipitate that was filtered and washed with H_2O and diethyl ether then dried *in vacuo* giving compound **9** as a yellow solid. Yield: 92%. ^{1}H NMR (300 MHz, CD_2Cl_2): δ 8.49 (d, 2H, *J* = 8.4 Hz), 8.13 (ddd, 2H, *J* = 7.5, 7.5, 1.5 Hz), 8.03 (ddd, 2H, *J* = 5.4, 1.5, 0.6 Hz), 7.97 (d, 2H, *J* = 7.8 Hz), 7.80 (dd, 2H, *J* = 7.5, 1.5 Hz), 7.76 (ddd, 2H, *J* = 9.0, 7.5, 0.9 Hz), 7.49 (ddd, 2H, *J* = 5.4, 1.5, 0.9 Hz), 7.46 (dd, 2H, *J* = 5.4, 1.2 Hz), 7.08 (ddd, 2H, *J* = 7.5, 7.5, 1.5 Hz) 6.93 (ddd, 2H, *J* = 7.5, 6.0, 1.5 Hz), 6.94 (ddd, 2H, *J* = 7.5, 7.5, 1.2 Hz), 6.31 (ddd, 2H, *J* = 7.5, 1.2, 0.6 Hz). HRMS (ESI-TOF) $[M]^+$: calcd for $C_{32}H_{24}IrN_4$ 657.1625, found 657.1638.

$[Ir(ppy)_2(4–NO_2–bpy)]PF_6$ (10): The synthesis of complex **10** was conducted in a manner similar to that of complex **9** with the exception of amounts used, $[Ir(ppy)_2Cl]_2$ (0.09 g, 0.09 mmol), and **1** (0.04 g, 0.2 mmol). Compound **10** was obtained as a brown-red solid. Yield: 79%. ^{1}H NMR (300 MHz, CD_2Cl_2): δ 9.09 (d, 1H, *J* = 2.1 Hz), 8.61 (d, 1H, *J* = 8.4 Hz), 8.33 (d, 1H, *J* = 6.3 Hz), 8.21 (ddd, 1H, *J* = 8.1, 8.1, 1.8 Hz), 8.11 (dd, 1H, *J* = 5.7, 2.1 Hz), 8.08 (d, 1H, *J* = 5.4 Hz), 7.97 (d, 2H, *J* = 8.1 Hz), 7.81 (ddd, 2H, *J* = 7.5, 7.5, 1.5 Hz), 7.76 (d, 2H, *J* = 7.8 Hz), 7.58 (ddd, 1H, *J* = 7.8, 5.4, 1.2 Hz), 7.54 (d, 1H, *J* = 6.0 Hz), 7.47 (d, 1H, *J* = 5.4 Hz), 7.03 (m, 6H), 6.32 (d, 1H, *J* = 7.2 Hz), 6.45 (d, 1H, *J* = 7.8 Hz). HRMS (ESI-TOF) $[M]^+$: calcd for $C_{32}H_{23}IrN_5O_2$ 702.1476, found 702.1474.

$[Ir(3T–ppy)_2(bpy)]PF_6$ (11): $[Ir(3T–ppy)_2Cl]_2$ (0.15 g, 0.050 mmol), and 2,2′–bipyridine (0.02 g, 0.1 mmol) were refluxed under an inert gas atmosphere in a 2:1 mixture of CH_2Cl_2:CH_3OH for 6 h. The reaction mixture was allowed to cool to r.t. and the solvent was removed by rotary evaporation. The sticky residue was sonicated in diethyl ether to give a solid that was filtered and washed with diethyl ether. The solid

was dissolved in CH_3OH and filtered before the addition of $NaPF_6$ (0.12 g) to the stirred solution. Concentration of the solution resulted in a precipitate that was collected by filtration and washed with H_2O then dried *in vacuo* to give compound **11** as an orange-brown solid. Yield: 51%. ^{1}H NMR (300 MHz, CD_2Cl_2): δ 8.52 (d, 2H, *J* = 8.1 Hz), 8.15 (ddd, 2H, *J* = 7.5, 7.5, 1.2 Hz), 8.08 (d, 4H, *J* = 6.0 Hz), 7.84 (d, 2H, *J* = 7.2 Hz), 7.62 (d, 2H, *J* = 3.9 Hz), 7.50 (t, 2H, *J* = 6.6 Hz), 7.44 (d, 2H, *J* = 6.3 Hz), 7.24 (d, 2H, *J* = 3.9 Hz), 7.17 (d, 2H, *J* = 3.6 Hz), 7.17 (d, 2H, *J* = 8.4 Hz), 7.12 (d, 2H, *J* = 8.4 Hz), 7.00 (ddd, 2H, *J* = 8.4, 8.4, 1.8 Hz), 6.95 (s, 4H), 6.78 (d, 2H, *J* = 3.6 Hz), 6.49 (d, 2H, *J* = 7.5 Hz), 2.78 (q, 8H, *J* = 8.4 Hz), 2.31 (s, 6H), 2.17 (s, 12H), 1.51 (m, 16H), 0.979 (t, 6H, *J* = 7.2 Hz), 0.937 (t, 6H, *J* = 7.2 Hz). HRMS (ESI-TOF) $[M]^+$: calcd for $C_{90}H_{88}IrN_4S_6$ 1609.4957, found 1609.4914.

$[Ir(3T–ppy)_2(4–NO_2–bpy)]PF_6$ (12): The synthesis of complex **12** was conducted in a manner similar to that of complex **11** with the exception of amounts used, $[Ir(3T–ppy)_2Cl]_2$ (0.09 g, 0.03 mmol), and **1** (0.01 g, 0.06 mmol). Compound **12** was obtained as an orange-brown solid. Yield: 51%. ^{1}H NMR (300 MHz, CD_2Cl_2): δ 9.12 (d, 1H, *J* = 2.1 Hz), 8.64 (d, 1H, *J* = 8.1), 8.38 (d, 1H, *J* = 5.7 Hz), 8.23 (ddd, 1H, *J* = 8.1, 8.1, 1.5 Hz), 8.14 (ddd, 1H, *J* = 6.0, 6.0, 2.4 Hz), 8.09 (s, 4H), 7.86 (d, 2H, *J* = 6.9 Hz), 7.63 (d, 2H, *J* = 3.9 Hz), 7.60 (d, 1H, *J* = 6.3 Hz), 7.48 (d, 1H, *J* = 6.3 Hz), 7.41 (d, 1H, *J* = 6.3 Hz), 7.24 (dd, 2H, *J* = 4.8, 0.9 Hz), 7.17 (d, 2H, *J* = 3.6 Hz), 7.15(m, 3H), 7.03 (q, 2H, *J* = 6.6 Hz), 6.95 (s, 4H), 6.78 (d, 2H, *J* = 3.6 Hz), 6.50 (d, 1H, *J* = 7.2 Hz), 6.46 (d, 1H, *J* = 7.5 Hz), 2.79 (q, 8H, *J* = 8.4 Hz), 2.31 (s, 6H), 2.17 (s, 12H), 1.50 (m, 16H), 0.977 (t, 6H, *J* = 7.2 Hz), 0.936 (t, 6H, *J* = 7.2). HRMS (ESI-TOF) $[M]^+$: calcd for $C_{90}H_{87}IrN_5O_2S_6$ 1654.4808, found 1654.4813.

Electrochemical Measurements. Electrochemical experiments were performed with a BAS 100B electrochemical analyzer using a standard three electrode setup consisting of a glassy-carbon working electrode, a platinum auxiliary electrode, and a Ag/AgCl reference electrode containing 1.0 M KCl. Supporting electrolyte tetrabutylammonium hexafluorophosphate ($TBAPF_6$, Sigma-Aldrich) was recrystallized from ethanol, dried and stored in a desiccator prior to use. All compounds studied by electrochemical analysis were prepared as 0.5 mM solutions in acetonitrile, dried over an activated alumina column and deaerated, containing 0.1 M $TBAPF_6$. Potentials are reported vs. aqueous Ag/AgCl and are not corrected for the junction potential. The $E^{\circ\prime}$ values for the ferrocenium/ferrocene couple for concentrations similar to those used in this study were +0.40 V for acetonitrile solutions at a glassy carbon electrode. A thorough description of the experimental setup and conditions used here has been described previously by our group.[24]

X–ray Structural Determination. The data for the structural determination were collected in the X–ray Crystallographic Lab in the LeClair-Dow Instrumentation Facility (Department of Chemistry, University of Minnesota). A single crystal of compound **10** was secured to a glass capillary and mounted on a Siemens SMART platform CCD diffractometer for a data collection at 173(2) K using a graphite monochromator and Mo Kα radiation (λ = 0.71073 Å). An initial set of cell constants was calculated from 51 reflections harvested from three sets of 20 frames such that orthogonal wedges of reciprocal space were surveyed. Final cell constants were determined from a minimum of 4023 strong reflections from the actual data collection. Data were collected to the extent of 1.5 hemispheres to a resolution of 0.77 Å. Four major sections of frames were

collected with 0.30º steps in ω. The intensity data were corrected for absorption and decay using SADABS.[25] The space group *Pnma* was determined based on systematic absences and intensity statistics. A direct-methods solution provided the positions of most non-hydrogen atoms. Full-matrix least squares/difference Fourier cycles were performed to locate the remaining non-hydrogen atoms. All non-hydrogen atoms were refined with anisotropic displacement parameters, and all hydrogen atoms were placed in ideal positions and refined as riding atoms with relative isotropic displacement parameters. All calculations were performed using the SHELXTL suite of programs.[26] Further details on the structural refinement and treatment of disordered solvent of crystallization and the NO_2 substituent are provided in the Supporting Information.

Optical Spectroscopy. Absorption spectra of the 3T oligomer and cationic Ir(III) bis-cyclometalates were collected for acetonitrile solutions using a 1.0 cm pathlength cell with a Cary 14 spectrophotometer running the OLIS globalworks software suite. Photoluminescence experiments were obtained using an excitation wavelength of 400 nm in acetonitrile using a front face geometry, with optical densities of solutions >2.0. Data was collected on a Spex Fluorolog 1680 0.2 m double spectrofluorimeter, equipped with a Hamamatsu R928 photomultiplier tube, running Datamax software. Solutions of the cationic Ir(III) bis-cyclometalates were deaerated for 15 minutes prior to collection using an argon purge. All spectra were corrected for the wavelength dependence of the detector. Luminescence quantum yields (ϕ_{em}) were measured relative to Coumarin 485 (C485) in acetonitrile solutions ($\phi_{em} = 0.28$), estimated uncertainties in ϕ_{em} measurements is ±20% or better.

Computational Details. All geometries were fully optimized using density functional theory (DFT) with the M06-L functional.[27] The 6-31G(d,p) basis set[28] was used for all non-metal atoms and the Stuttgart/Dresden (SDD) basis set[29] relativistic effective core potential was used for the Ir(III) metal centers. The *n*–Bu groups found in the 3′ and 4′ positions of the terthiophene pendants were replaced with hydrogen atoms for all computations. No symmetry restrictions were imposed while determining the fully optimized ground state geometries. Integral evaluation made use of the grid defined as ultrafine in the Gaussian 09 program.[30] The nature of all stationary points was verified by analytic computation of vibrational frequencies.[31] Solvent effects for acetonitrile were modeled with SMD.[32] To obtain the vertical excitation energies of the three lowest singlet and triplet excited states of the studied complexes time-dependent DFT (TD-DFT)[33] calculations were performed using the M06-2X functional[34] at the M06-L optimized ground-state (S_0) geometry. Acetonitrile non-equlibrium solvatochromic effects were evaluated via a linear response formalism using SMD cavities.[33a]

Results and Discussion

Synthesis of Ligands and Complexes. Syntheses of the 3T oligomer **6**, its corresponding Ir(III) complexes **11** – **12**, and the Ir(III) control complexes **9** – **10** are outlined in Scheme 1. The diimine ligand 4–nitro–2,2′–bipyridine (**1**)[21], precursor 4–bromo–2–phenylpyridine (**2**)[22] and 5–bromo–3′,4′–dibutyl–2,2′:5′,2″–terthiophene (**3**)[23] were synthesized with slight modifications to previously reported literature procedures. Compound **3** was reacted with mesitylboronic acid ((Mes)B$(OH)_2$) under Suzuki coupling conditions to obtain the mono-mesityl-capped terthiophene **4** in good yield (82%). The mono-stannylated terthiophene **5** was prepared in quantitative yield by

reaction of the mono-lithiated derivative of **4**, generated *in situ*, with tributyltin chloride. Compound **5** was then coupled to **2** using standard Stille coupling conditions to obtain the desired cyclometalating 3T oligomer **6** in good yield (78%).

Scheme 1. Synthesis of 3T-ligand and cationic Ir(III) bis-cyclometalates.

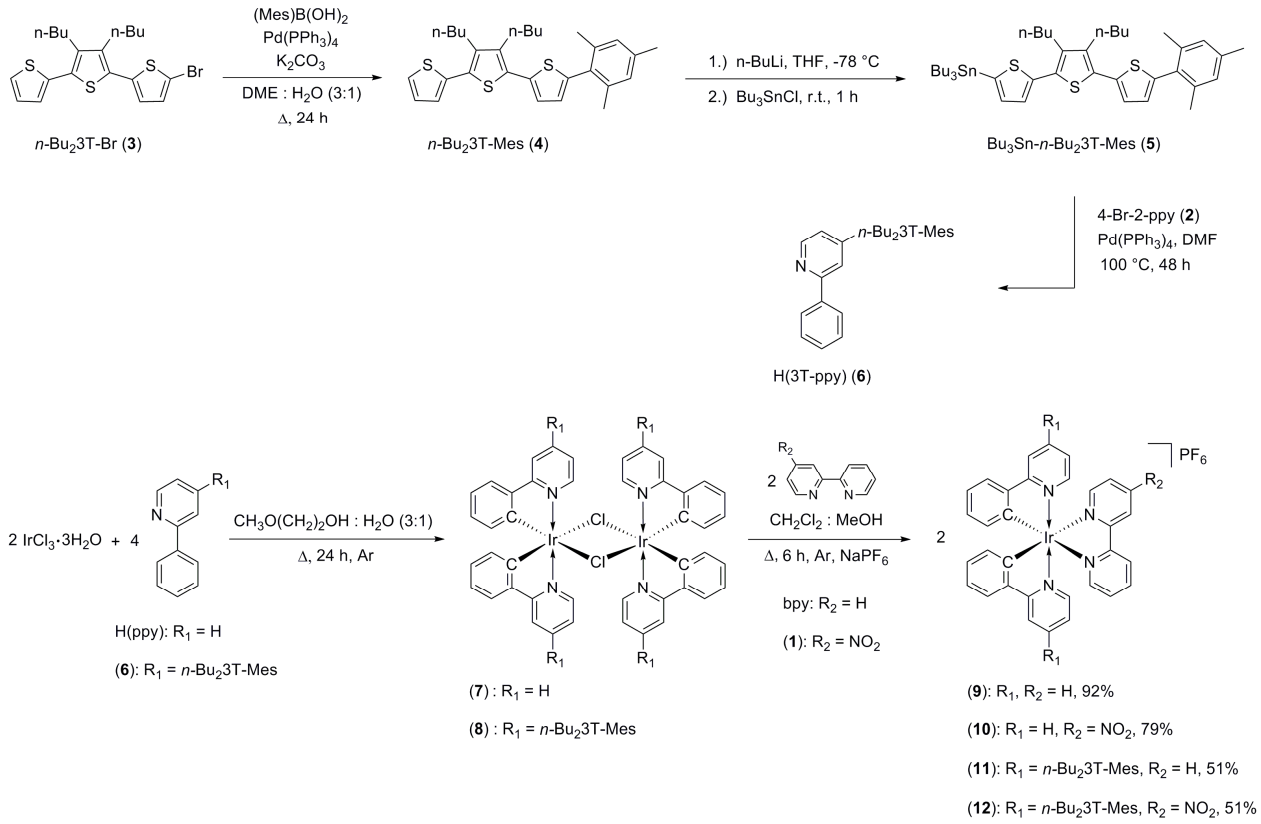

The desired series of complexes **9** – **12** were synthesized via conventional synthetic procedures for cationic Ir(III) bis-cyclometalates, with control complexes **9** – **10** (79 – 92%), and the 3T–pendant complexes **11** – **12** (51%), isolated in good to moderate yields. The dichloro–bridged dimers $[Ir(C\hat{}N)_2(\mu\text{–}Cl)]_2$ **7** and **8**, were prepared using the method described by Watts *et al.*, substituting 2–ethoxyethanol for 2–methoxyethanol.[20] Dimers **7** and **8** were cleaved with the appropriate diimine ligand in a mixture of refluxing CH_2Cl_2:MeOH (1:1 for the synthesis of **9** an **10** and 2:1 for the synthesis of **11**

and **12**) to generate the monomeric $[Ir(C^N)_2(N^N)]^+$ species as Cl^- salts. These salts were subsequently metathesized by treatment with $NaPF_6$ to give PF_6^- as the counterion.[2a] Complexes **9** – **12** were characterized by ^1H NMR spectroscopy as well as HR–ESI mass spectrometry. Ir(III) complexes **9** – **12** display ^1H NMR spectra consistent with a C,C–*cis* / N,N–*trans* coordination mode for the cyclometalating ligands. As expected for molecules of C_2 symmetry, **9** and **11** show a single resonance for each set of aromatic ^1Hs, 12 total for **9**, and 15 total for **11**. Complexes **10** and **12** display more complicated ^1H NMR spectra as introduction of the NO_2 substituent results in a loss of symmetry. The number of ^1H signals observed for the aromatic region is increased, 15 total for **10**, and 19 total for **12**. In the case of **10** further confirmation of structural assignment was provided by single crystal X–ray crystallography.

X–ray Crystallography. Single crystals of **10** were grown by slow evaporation from a CH_2Cl_2 solution. Relevant crystallographic data for **10** is shown in Table 1, a list of selected bond lengths and angles (experimental and calculated) can be found in Table 2. The structure obtained for **10** displays two ppy cyclometalating ligands in the C,C–*cis* / N,N–*trans* or "*mer* like" arrangement about a pseudo-octahedrally coordinated Ir(III) ion (Figure 2). The 4–NO_2–bpy diimine ligand occupies the remaining two coordination sites with both N atoms *trans* to the carbanions of the ppy ligands. Ir(III)–ligand bond lengths for the diimine and cyclometalating ligands are in good agreement with distances found for similar $[Ir(C^N)_2(N^N)]^+$ species.[2b, 7e, 9p, 16b, 35] As is typically observed within cyclometalating ligands the Ir–C bonds (~2.02 Å) are slightly shorter than those of the Ir–N bonds (~2.04 Å), while the Ir–N bonds (~2.14 Å) to the diimine ligand are longer than those observed for the cyclometalating ligands (Table 2). Lengthening of the $Ir–N_{(N^N)}$ is

regularly observed in these complexes due to the strong *trans*-influence of the cyclometalated carbanions.[2b, 7e, 9p, 16b, 35]

A search of the Cambridge Crystallographic Database (CSD)[36] indicates **10** is the first Ir(III) species among five transition metal complexes to contain a NO_2 functionalized bipyridine ligand to be characterized crystallographically.[37] Surprisingly the presence of a NO_2 substituent on the diimine ligand appears to have no observable effect on the Ir1–N4 or the Ir1–C11 distances. The average N–O bond length found for atoms O1, O2 and N5 is 1.220(11) Å, which compares well with the average values attained from the CSD[36] (1.213(12) Å) and the DFT optimized ground state geometry (1.229 Å). The NO_2 substituent was nearly coplanar with the bpy ligand, with a small torsion angle of 10.6(4)°, as measured from the O2–N5–C25–C24 unit. A slight twist in the NO_2 substituent is commonly observed for transition metal complexes with NO_2 functionalized phenanthroline and bipyridine ligands in the coordination sphere.[37b, 38]

Table 1. Crystallographic Data and Refinement Parameters for $[Ir(ppy)_2(4–NO_2–bpy)]PF_6$ (**10**).

empirical formula	$C_{32}\ H_{23}\ F_6\ Ir\ N_5\ O_2\ P$
crystal color, morphology	red–orange, plate
crystal system	Orthorhombic
space group	*Pnma*
a, Å	21.287(4)
b, Å	26.420(5)
c, Å	13.113(3)
α, deg	90
β, deg	90
γ, deg	90
Volume (*V*), Å^3	7375(2)
Z	8
formula weight, g mol^{-1}	731.76
density (calculated), g cm^{-3}	1.525
temperature, K	173(2)
absorption coefficient (μ), mm^{-1}	3.728
F(000)	3296
θ range, deg	1.54 to 27.51
index ranges	$-27 \le h \le 27$
	$-34 \le k \le 34$
	$-17 \le l \le 16$
reflections collected	75379
independent reflections	8645 [R_{int} = 0.1145]
weighting factors,[a] *a, b*	0.0493, 11.7270
max, min transmission	0.9126, 0.3316
data/restraints/parameters	8645/3/446
R_1, wR_2 [$I > 2\sigma(I)$]	0.0548, 0.1038
R_1, wR_2 (all data)	0.1095, 0.1181
GOF	1.052
largest diff. peak, hole eÅ^{-3}	1.037, –0.788

[a] $w = [\sigma^2(F_o^2) + (aP)^2 + (bP)]^{-1}$, where $P = (F_o^2 + 2F_c^2)/3$.

Table 2. Selected Bond Lengths and Angles for $[Ir(ppy)_2(4–NO_2–bpy)]PF_6$ (**10**).

	Bond Length (Å)			Bond Angle (°)	
Atoms	Experimental	Calculated	Atoms	Experimental	Calculated
Ir1 – N1	2.043(5)	2.087	N1 – Ir1 – C22	80.7(2)	79.8
Ir1 – N2	2.038(5)	2.089	N2 – Ir1 – C11	79.6(3)	79.7
Ir1 – N3	2.137(5)	2.217	N3 – Ir1 – N4	76.5(2)	74.2
Ir1 – N4	2.139(5)	2.209	O1 – N5 – O2	124.7(7)	125.1
Ir1 – C11	2.031(6)	2.018			
Ir1 – C22	2.013(7)	2.020			
N5 – O1	1.240(8)	1.229			
N5 – O2	1.199(8)	1.229			

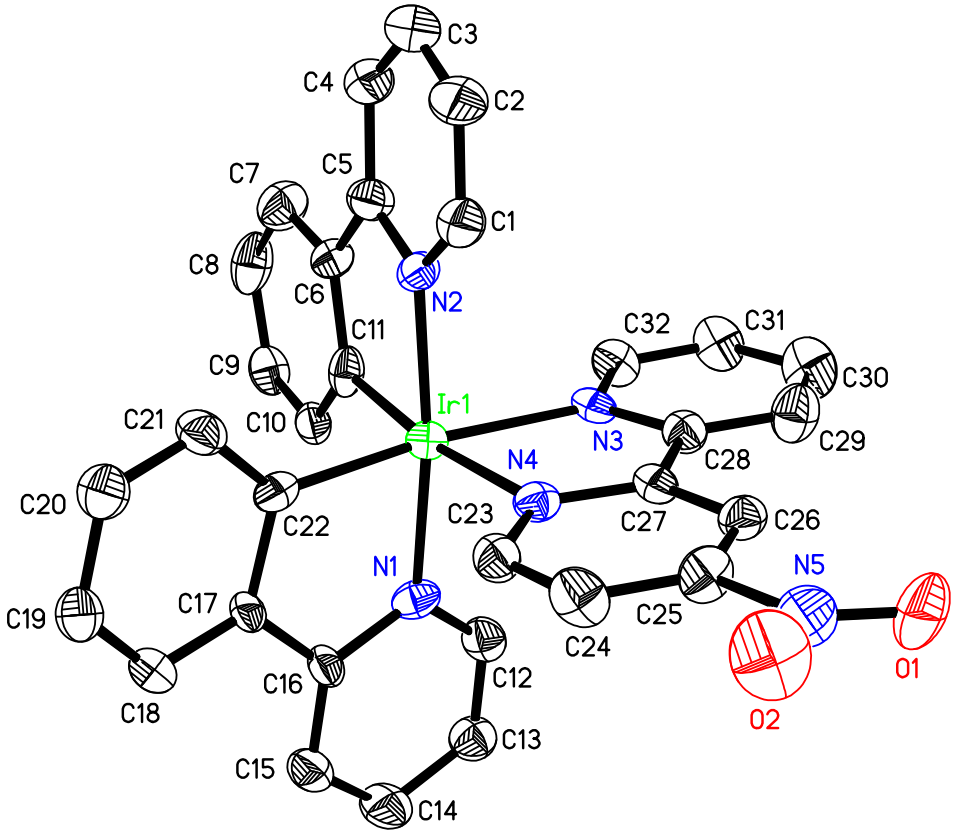

Figure 2. Thermal ellipsoid plot of $[Ir(ppy)_2(4–NO_2–bpy)]PF_6$ (**10**). Major component of disordered NO_2 substituent is shown. Hydrogen atoms, and PF_6^- counterion have been removed for clarity.

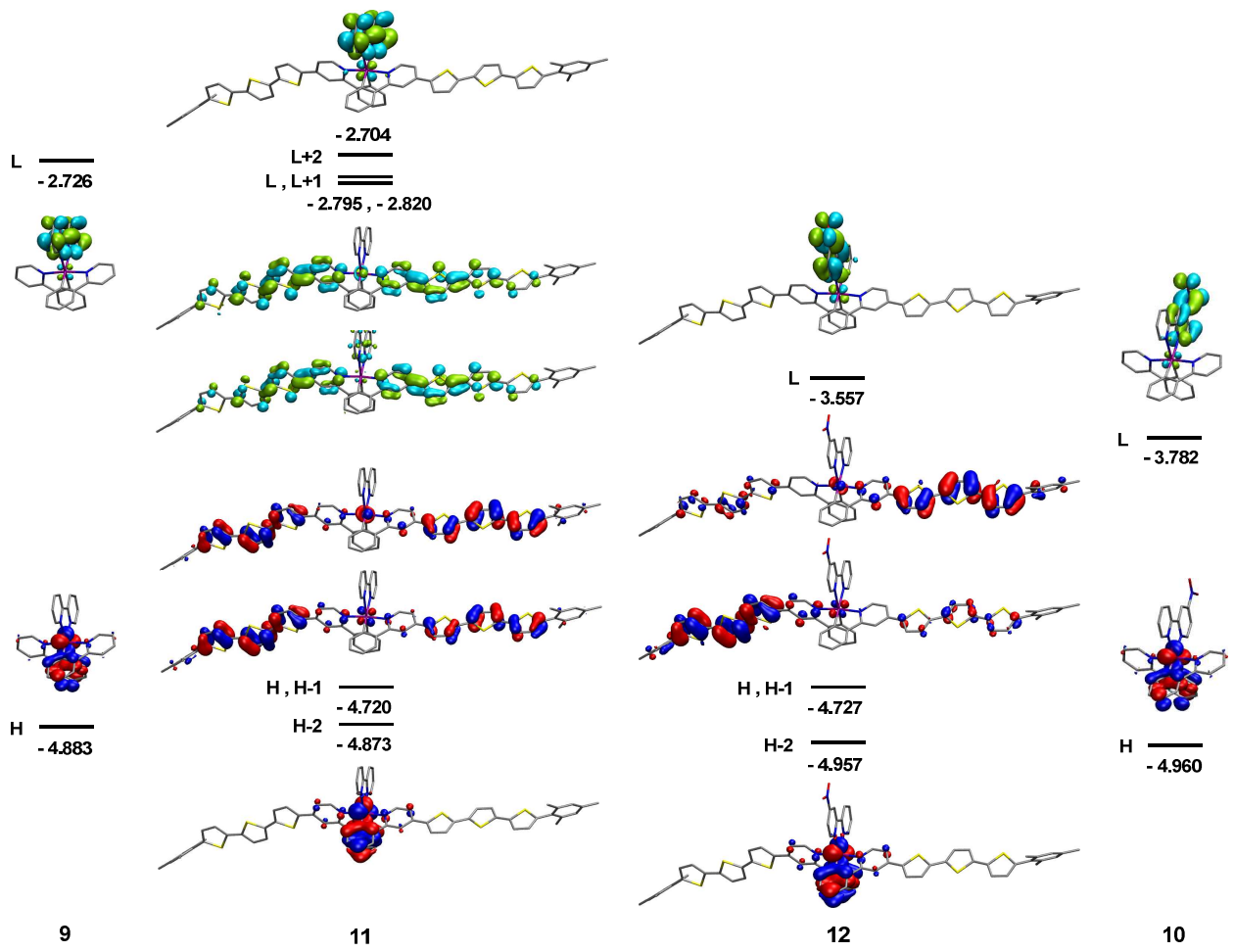

Figure 3. Contour plots of frontier orbitals (0.002 a.u.) for control complexes (**9** – **10**) and 3T–pendant complexes (**11** – **12**) in the ground state. Occupied orbitals are shown in blue/red, virtual orbitals are in cyan/green. Hydrogen atoms omitted for clarity.

Frontier Orbital Analysis. Theoretical calculations were performed in support of experiment to assess the optimized ground state geometry and electronic structure of both the control (**9** – **10**) and 3T–pendant (**11** – **12**) complexes. Calculations at the DFT level of theory allowed the investigation of the stepwise addition of 3T–pendants and NO_2 substituents. Contour plots representing the frontier orbitals for the series (**9** – **12**) can be found in Figure 3. Control complexes **9** and **10** exhibit electron density assigned to the HOMO localized over the Ir(III) ion and the phenyl ring of the cyclometalating ligands. The HOMO is virtually unchanged on addition of the NO_2 substituent. The

LUMO is found to reside almost exclusively on the π–system of the diimine ligand (bpy/4–NO_2–bpy) in **9** and **10**, greatly stabilized by the NO_2 substituent.

Addition of 3T–pendants to complexes **11** and **12** does little to affect the energy or nature of the molecular orbital (MO) localized on the Ir(III)–$(Ph^{-}_{C\wedge N})_2$ moiety, assigned as the HOMO−2 in the 3T–pendant complexes (Figure 3). In both complexes **11** and **12** calculations show a higher lying pair of degenerate MOs representing the HOMO and HOMO−1 delocalized over the 3T π–system. The small contribution of electron density to the HOMO or HOMO−1 from the cyclometalating ligand cap indicates poor interaction between the 3T–pendant and the Ir(III) ion in the ground state.

Analysis of the lowest unoccupied orbitals for the series (**9** – **12**) shows a MO of similar composition localized on the diimine ligand. These MOs are assigned as the LUMO in **9** and the LUMO+2 in **11**, while the diimine based MOs on the NO_2 functionalized compounds are greatly stabilized, leading to their assignment as LUMO in both **10** and **12**. For the 3T–pendant complexes **11** and **12**, calculations show a pair of nearly degenerate MOs delocalized over the 3T–pendant and pyridyl ring of each cyclometalating ligand. In the case of **11**, these orbitals (LUMO/LUMO+1) lie close in energy to the diimine based MO, while in complex **12** these orbitals (LUMO+1/LUMO+2) are significantly higher in energy (-2.833 eV, not shown) than the NO_2 stabilized diimine MO.

Table 3. Photophysical[a] and Electrochemical[b] Properties of 3T oligomer **6** and Cationic Ir(III) Complexes **9** – **12**.

				$E_{1/2(ox)}$, V		$E_{1/2(red)}$, V
Compound	$\lambda_{abs,}$ nm	$\lambda_{em,}$ nm[c]	ϕ_{em}[d]	Ir(IV)/Ir(III)[e]	$3T^{\cdot+}/3T$	$bpy/bpy^{\cdot-}$
6	252, 378	498	0.11	—	1.04	—
9	255, 265, 312, 344 375, 415, 470	603	0.11	1.29	—	– 1.37
10	252, 266, 305, 381 400, 530	599	0.005	1.35	—	– 0.52
11	263, 300, 421	579, 756	0.001	1.36	1.10	– 1.25
12	263, 308, 418	592	0.0003	1.38	1.10	– 0.40

[a] Spectra recorded in ACN solutions. [b] Potentials measured vs Ag/AgCl 1.0 M KCl at room temperature in dry degassed 0.1 M $TBAPF_6$ ACN solution, scan rate 100 mV/s. [c] Deaerated solutions at 298 K, $\lambda_{ex} = 400$ nm. [d] Determined relative to Coumarin 485 in ACN ($\phi_{em} = 0.28$). [e] Redox couple also contains significant contribution from the cyclometalating ligands.

Electrochemistry of the Control Complexes. The electrochemical properties of the cationic Ir(III) bis-cyclometalates (**9 – 12**) investigated here are in agreement with the DFT simulations discussed above. Results of the electrochemical investigation in acetonitrile (ACN) for control complexes **9** and **10** are given in Table 3 and Figure 4. Both complexes **9** and **10** displayed electrochemical behavior typical of $[Ir(C^N)_2(N^N)]^+$ type complexes.[4g, 7e, 8j, 9d, 9n, 10] Quasi-reversible single electron processes within the solvent window were observed for **9** and **10**, centered at 1.29 and 1.35 V respectively. Addition of the NO_2 substituent causes a nominal positive shift (60 mV) in the oxidation of **10** relative to **9**, consistent with the minimal disturbance in their HOMO energies, as predicted by DFT. A single reduction centered at −1.37 V for complex **9**, is replaced by two reductions for complex **10**, centered at −0.52 and −1.16 V. A third reduction at −1.42 V may be due to the successive reduction of the doubly

reduced species. These reductive processes are assigned to ligand based reductions of the diimine ligand found in **9** and **10**.

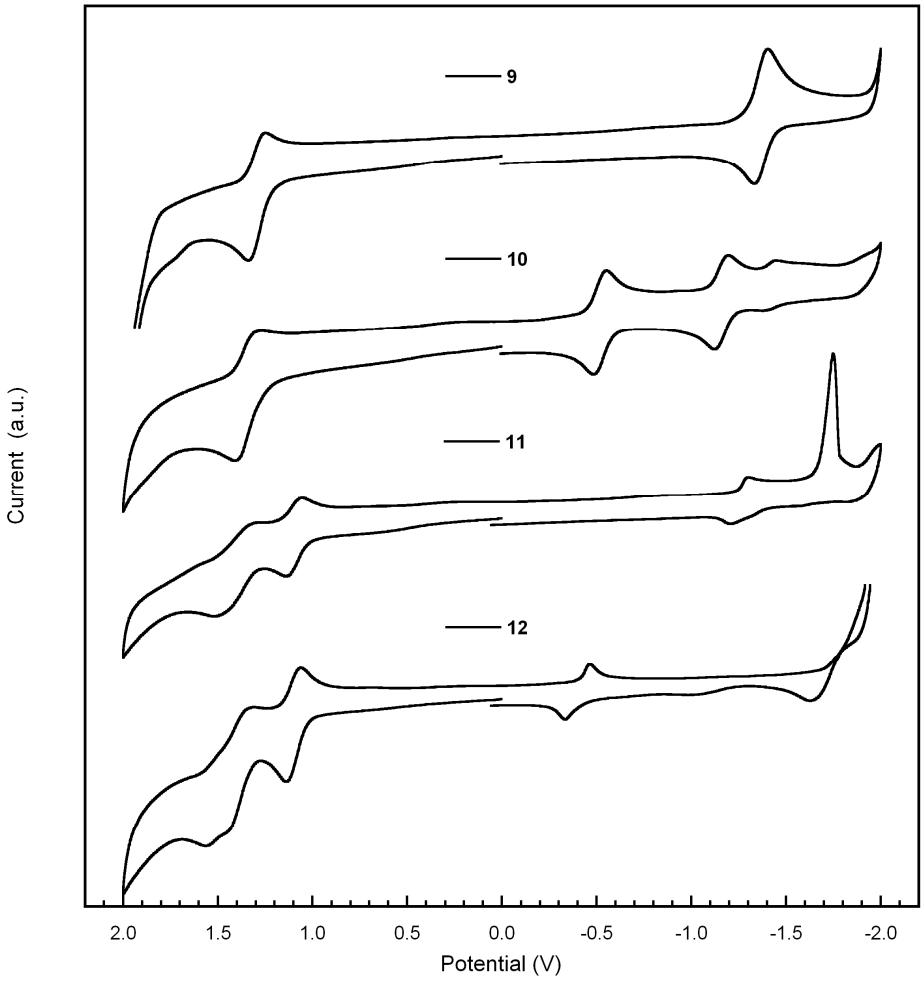

Figure 4. Cyclic voltammograms in ACN for control complexes **9**, **10** and 3T–pendant complexes **11**, **12**. Anodic currents are positive and plotted downward. Scan rate of 100 mV/s.

The most notable difference between the electrochemistry of the control complexes is the large positive shift (850 mV) in the first reduction of **10** relative to **9**. Significant perturbation of the first reduction potential and LUMO energy of **10** clearly demonstrates the strong electron withdrawing character of the NO_2 substituent. A positive shift in the location of the first reductive process is well documented for similar

complexes coordinating NO_2 substituted ligands, although the terminus of the electron has been a topic of debate.[9d, 39] Recent work to determine the reduction site of 4–NO_2–bpy (**1**) and its Pt(II) coordination complex Pt(4–NO_2–bpy)Cl_2 was conducted by Murray *et al.* with a combination of theoretical calculations, cyclic voltammetry, as well as UV/vis, NIR, and EPR spectroelectrochemistry.[40] Their results indicate that after electrochemical reduction or photoexcitation (MLCT, $d\pi_{Pt(II)} \rightarrow \pi^*_{N\wedge N}$) the major component of electron density is localized on the NO_2 substituted pyridyl ring in both the bound and unbound ligand. We adopt their assignment for the first reduction in complex **10** as the one electron reduction of the NO_2 substituted pyridyl ring of the coordinated 4–NO_2–bpy ligand. It is likely that the reduction at more negative potentials in **10** is the addition of the second electron to the unsubstituted pyridyl ring, slightly stabilized by induction.

Electrochemistry of the 3T oligomer and 3T–pendant Complexes. The electrochemical properties of the 3T oligomer **6** and its corresponding Ir(III) complexes **11** and **12** were also examined in ACN by cyclic voltammetry (Table 3, Figure 4). No reductions were observed for the 3T oligomer within the solvent window, as expected for similar aryl capped terthiophene species,[14b, 14e, 14g] but the oligomer did exhibit rich oxidation chemistry, undergoing two reversible, and one quasi-reversible oxidation processes. The first 3T oligomer oxidation is centered at 1.04 V, and is assigned to the formation of the 3T radical cation.[13e, 14b, 14c, 14e, 14f] Further oxidation produces a dicationic species.

As observed for complexes **9** and **10**, each of the 3T–pendant complexes undergoes a quasi-reversible reduction located at −1.25 and −0.40 V respectively for **11**

and **12**. Generation of more highly reduced species at more negative potentials during electrochemical experiments conducted with **11** and **12** gave evidence for precipitation on the electrode surface. These additional reductions were not assigned. A noteworthy similarity in the electrochemical data is the 850 mV positive shift observed for the first reduction of the diimine ligand in the NO_2 functionalized **10** and **12**, relative to complexes **9** and **11**. The similarity in the reduction chemistry of the 3T–pendant complexes is fully supported by computational results, which present diimine MOs nearly identical to those of the analogous control complexes.

The 3T–pendant complexes **11** and **12** revealed three oxidation processes rather than the single process observed for the control complexes **9** and **10** (Table 3). In the 3T–pendant complexes the first quasi-reversible oxidation at 1.10 V is assigned to the isopotential one electron oxidation of both 3T–pendants to form the respective 3T radical cations. This process is nearly unchanged in potential from the analogous process in the free 3T oligomer, suggesting the ground states of the 3T–pendant complexes and 3T oligomer are comparable. The second process at ~ 1.37 V is assigned to the oxidation of the Ir(III)–$(Ph^{-}_{C\wedge N})_2$ moiety, only slightly shifted from the values observed for the same process in control complexes (Table 3). The third oxidation process located at ~ 1.54 V is attributed to a second oxidation of the 3T–pendant to form the dicationic terthiophene species.[13e, 14b, 14e, 24] This process is not reversible on the CV time scale and occurs at potentials close to the second oxidation making it difficult to resolve electrochemically. Ordering of the first two oxidative processes are in accord with the composition of the HOMO/HOMO–1, and HOMO–2 predicted by DFT calculations.

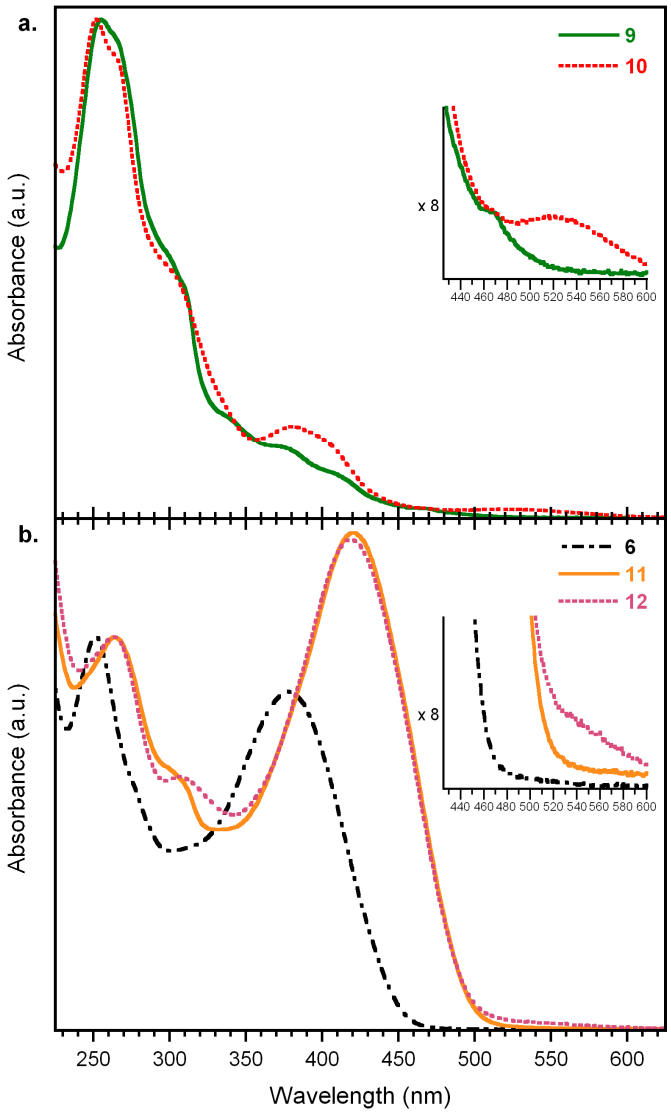

Figure 5. Normalized UV-vis absorption spectra in ACN solutions at room temperature of (a) control complexes **9**, **10**. (b) 3T oligomer **6** and 3T-pendant complexes **11**, **12**. Insets depict long wavelength absorbance of **10** and **12**.

Electronic Spectroscopy and Excited State Analysis. UV-vis absorption spectra collected in ACN for cationic Ir(III) bis-cyclometalates **9** – **12**, and the free 3T oligomer **6**, are shown in Figure 5. Corresponding photophysical and spectral data have been summarized in Table 3. To assist with the interpretation of excited state properties, TD-DFT calculations were performed for all molecules in the series (**9** – **12**) on their fully-optimized ground-state geometries. An energy level diagram representing the three lowest singlet and triplet excited states of complexes **11** and **12** is shown in Figure 6 (see Supporting Information for detailed assignment of states). The free 3T oligomer exhibits a relatively simple electronic spectrum with only two strongly absorbing features. The high energy band, located at 252 nm, is assigned to the $\pi \rightarrow \pi^*$ transition localized on the Hppy cap of **6**. The broad, intense absorption at lower energy (378 nm) is identified as the $\pi \rightarrow \pi^*$ transition characteristic of π–conjugated thiophene oligomers.

Control complexes **9** and **10** presented absorption spectra representative of comparable cationic Ir(III) bis-cyclometalates.[2a, 4h, 7e, 9b, 9e, 9n, 10a, 41] Vertical excitations to the lowest energy singlet state S_1 in the control complexes are described as a mixed ^{1}LLCT/^{1}MLCT transition by TD-DFT, computed to occur at 326 (**9**) and 388 (**10**) nm. Experiment shows intense absorption bands and shoulders present at high energy (320 – 350 nm), assigned to ^{1}LC transitions ($\pi \rightarrow \pi^*$) on the cyclometalating and diimine ligands. At lower energy a series of weak absorption shoulders (340 – 440 nm) followed by a set of very weak absorptions (450 – 470 nm) can be found. The bands located between 340 – 440 nm are assigned to ^{1}LLCT/^{1}MLCT transitions ($\pi_{ph-} \rightarrow \pi^*_{N\wedge N}/d\pi_{Ir(III)} \rightarrow \pi^*_{N\wedge N}$), while those found at wavelengths longer than 450 nm likely result from transitions to the corresponding triplet states. The exact ordering of these bands is not

known for complexes **9** and **10**. The long wavelength absorption band centered at 530 nm for complex **10** is likely due to transitions terminating on the significantly stabilized MO of the NO_2 substituted diimine ligand (see inset Figure 5).

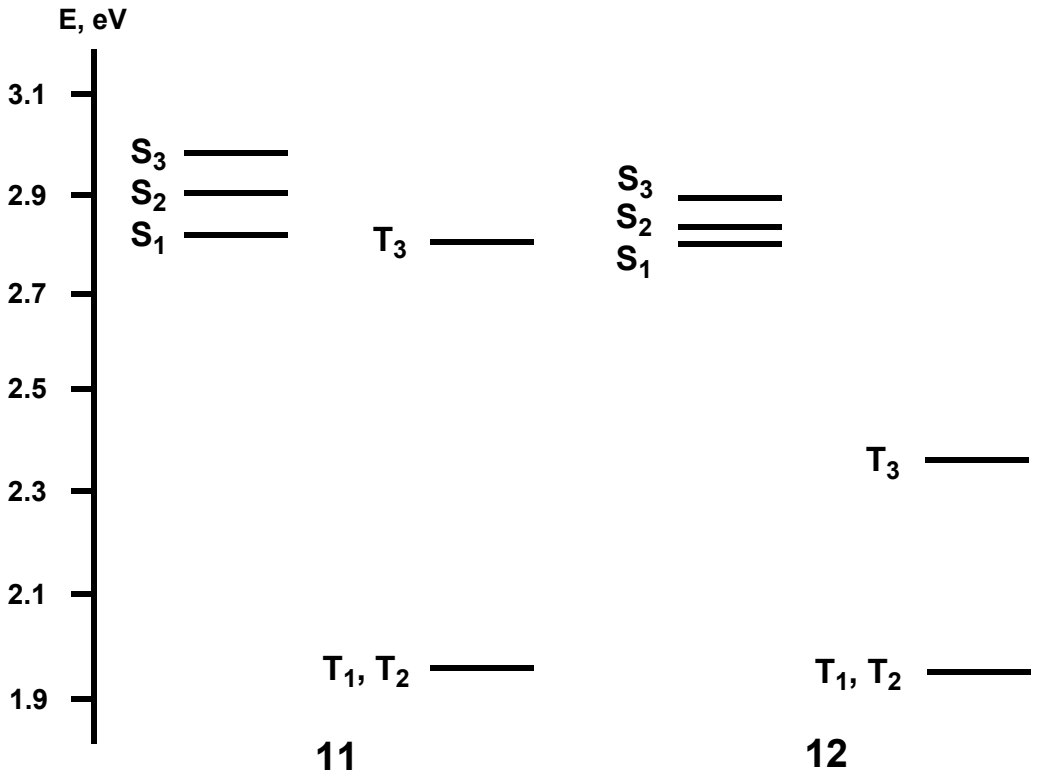

Figure 6. Energy level diagram for the lowest excited states in the 3T–pendant complexes (**11** – **12**).

Interpretation of the electronic spectra for the 3T–pendant complexes **11** and **12** becomes increasingly more complicated than for either the 3T oligomer or the control complexes. Vertical excitations to the lowest energy singlet state S_1 in the 3T–pendant complexes are described as a $^1\pi \rightarrow \pi^*$ transition by TD-DFT. Calculated values for excitation of the S_1 state are 446 (**11**) and 448 (**12**) nm. Experimentally the ultraviolet region of complexes **11** and **12** display the same intense high energy absorptions as **9** and **10**, consistent with the ^{1}LC transitions ($\pi \rightarrow \pi^*$) on the cyclometalating and diimine

ligands. The remaining portions of the spectra are dominated by the characteristic $^1\pi \rightarrow \pi^*$ transition of the 3T–pendants, as observed in the 3T oligomer. The absorbance of this band is also increased (~ x1.5) due to the existence of two 3T–pendants within the same molecule. Presence of the NO_2 substituent on the diimine ligand of **12** yields a long wavelength absorption near 540 nm analogous to the band observed in **10**. The NO_2 substitution appears to have no effect on the overall position of the absorption bands corresponding to the 3T–pendants. The broad absorptions attributed to the 3T–pendants in complexes **11** and **12** overlap substantially with the position of the charge transfer bands observed in the control complexes. Observation and assignment of those bands expected to be present beneath the 3T–pendant absorptions would require additional experiments and data treatment beyond the scope of this study.

A noteworthy red-shift (~ 40 nm) in the absorption of the 3T–pendants $^1\pi \rightarrow \pi^*$ transition is observed upon complexation of **6** to the Ir(III) ion in both **11** and **12**. Behavior such as this has been consistently observed for coordination of ligands functionalized with oligothiophene pendants to transition metal centers,[13h] rationalized as stabilization of the oligothiophene excited state resulting from increased conjugation with the aryl caps along with the metal cations inductive effect.[24b] We believe this reasoning can be applied as the likely cause of the red-shift described here for complexes **11** and **12**.

Aside from complex **9**, whose luminescence has been previously reported,[2a, 9b, 9e, 9n, 10b, 41a, 41e] the remaining cationic Ir(III) bis-cyclometalates display extremely weak luminescence at room temperature. Quantum yields obtained for the NO_2 and 3T functionalized compounds are 2 – 3 orders of magnitude smaller than that of control complex **9**. In the case of the 3T–pendant complexes accurate measurement of quantum

yield or time dependent decay dynamics using our experimental configuration were not possible due to extremely low luminescence intensities.

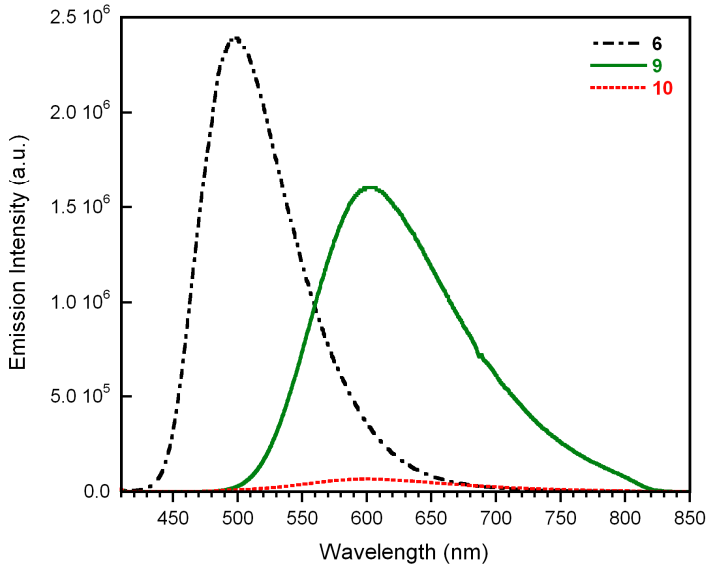

Figure 7. Luminescence spectra of 3T oligomer **6** and control complexes **9**, **10** in deaerated ACN solutions at 298 K. λ_{ex} = 400 nm.

The experimentally observed luminescence of control complexes **9** and **10** (Table 3, Figure 7) is described by TD-DFT as an excitation to the lowest triplet excited state T_1 with ^{3}LLCT/^{3}MLCT character, computed to arise at 381 (**9**) and 524 (**10**) nm. For the non-luminescent 3T–pendant complexes TD-DFT predicts excitations to the 3T centered T_1 and T_2 states (Figure 6), a degenerate pair of low lying triplet states, $^3\pi \rightarrow \pi^*$ in character. Calculations place the energy of these degenerate triplet states 1.96 eV above the ground. This value is in excellent agreement with the values measured and computed for the lowest triplet excited state of the unfunctionalized 3T oligomer, ranging from 1.76 – 1.92 eV.[42]

A partial decrease in emission intensity has been observed for Ir(III) complexes similar to **10** coordinating electron withdrawing diimine ligands bearing COOH or

COOR substituents.[4h, 7e, 9p] In cases where the strong electron withdrawing NO_2 substituent is used, near total quenching of charge transfer phosphorescence is reported for Ru(II), Re(I), Pt(II), and Ir(III) species.[9d, 39a, 43] Strong involvement of the NO_2 substituent with the excited state and its vibrational modes are believed to be the major deactivation pathway of radiative decay in **10**.[39a] There is also evidence in NO_2 aromatics for excited state deactivation due to structural reorganization, involving intramolecular twisting of the NO_2 substituent out of the aromatic ring plane.[44] The weak emission measured for **10** is in nearly the same location as that of control complex **9** (Table 3). Electrochemical measurements and analysis of absorption band energies for **10** suggest excitation of the ^{1}LLCT/^{1}MLCT state and subsequent decay from the ^{3}LLCT/^{3}MLCT after rapid intersystem crossing to occur at much lower energies than observed. Considering the position and the extremely low quantum yield we cannot be certain of the origin of luminescence from **10**; for example, the luminescence may originate from an alternate triplet state on the diimine ligand. In any event, efficient deactivation of excitation energy likely occurs through a triplet state partially localized on the NO_2 substituent.

Discussion. Electrochemistry and DFT calculations for the first oxidation and reduction processes in complexes **9** and **10** correlate with the relative positioning of the HOMO and LUMO, respectively. From the electrochemical and theoretical results, it is reasonable to infer that the HOMO in complex **10** is relatively undisturbed by the NO_2 substituent. Conversely, the very large shift in the reduction potential and computed energy of the LUMO for **10** suggests significant stabilization of this MO, as has been previously reported.[9d, 39-40] These results emphasize the ability to independently modify

the energy of HOMO and LUMO. Specific functionalization of the cyclometalating and diimine ligands then allows for the potential to create a low lying trap state for triplet energy.

Introduction of 3T–pendants into the system provides additional photoredox chromophores with MOs that may produce dramatic changes in the excited state dynamics. Relative to both the control complexes and the 3T oligomer an overall positive shift for the oxidation of the 3T–pendants and the Ir(III)–$(Ph^{-}_{C\wedge N})_2$ moiety in complexes **11** and **12** is apparent, but minimal. The minimal disturbance in the oxidation potential of the 3T–pendants is indicative of minor electronic involvement between the 3T and Ir(III) chromophores in the ground state. Further evidence of the weak interaction is found in the contour plots of the HOMO/HOMO−1 for complexes **11** and **12**. This type of weak electronic coupling is commonly observed in metal-oligothiophene systems, attributed to decreased conjugation between the ligated aryl caps and their oligothiophene pendants.[24b, 45] This suggests that coordination of the ligand containing the 3T oligomer is unlikely to be a significant contributor to the changes in the electrochemical processes observed at positive potentials. Rather, this shift to positive potentials is likely a consequence of the increased positive charge imparted on the complexes through sequential oxidation.

The 3T–pendants have a more pronounced effect on the excited states of complexes **11** and **12**. The absence of strong luminescence from the 3T–pendant complex **11** is striking as both the free 3T oligomer **6** and the control compound **9** display strong fluorescence and phosphorescence respectively, both with $\phi_{em} = 0.11$. For uncoordinated oligothiophene chromophores fluorescence from the initial photoexcited $^1\pi - \pi^*$ state is

observed, with intersystem crossing to the lowest energy nonemissive $^3\pi - \pi^*$ state representing the major non-radiative pathway.[42a] It has also been shown that asymmetric capping of 3T oligomers in the 5 or 5″ position with electron withdrawing substituents enhances the rate of non-radiative decay (k_{nr}) in polar solvents by imparting a charge transfer character from the 3T–backbone to the polarized caps, deactivating fluorescence from the $^1\pi - \pi^*$ state.[14d] In complex **11** the presence of a positively charged Ir(III) ion coordinated to the ppy cap of the 3T oligomer serves as electron withdrawing moiety in the excited state, as indicated by the significant contribution from the pyridyl ring of the cyclometalating ligands in the contour plot of the LUMO/LUMO+1.

Based on TD-DFT results and the disparity between the extinction coefficients of the 3T and Ir(III) chromophore, photoexcitation of the 3T–pendant complexes efficiently populates the 3T $^1\pi - \pi^*$ state, although contributions of a charge transfer character cannot be mutually excluded. We suggest that following photoexcitation, the $^1\pi - \pi^*$ state rapidly undergoes intersystem crossing to the lowest energy excited triplet state facilitated by the strong spin-orbit coupling of the Ir(III) ion. TD-DFT finds the lowest energy excited state to be the 3T based $^3\pi - \pi^*$ state, where the excitation energy is left to decay non-radiatively.[8a, 46] Existence of the dark $^3\pi - \pi^*$ states below the potentially emissive Ir(III) based triplet states found in the control complexes further supports deactivation of potential radiative decay pathways. This relative positioning of excited triplet states has been observed in other metal-oligothiophene systems, resulting in quenching of oligomer fluorescence and metal centered phosphorescence, supporting the quenching observed here.[13a, 13b, 13j, 46a]

The 3T/NO_2 functionalized compound **12** is similar to **11** and its photophysical behavior can be rationalized using the arguments outlined above for both complexes **10** and **11**. In summary, attempts to design a trap for the lowest triplet excited state through functionalization of the diimine ligand with a NO_2 substituent did not lower the energy of the diimine MO (Figure 7, T_3 for **12**) enough to shift the resulting ^{3}LLCT/^{3}MLCT state below the 3T $^3\pi - \pi^*$ state. As a result it is no surprise that neither fluorescence nor phosphorescence is observed in the 3T–pendant complexes.

Conclusions. We have carried out electrochemical and photophysical investigations that include theoretical calculations on a series of cationic Ir(III) bis-cyclometalated complexes (**9** – **12**) incorporating 3T–pendants and the potent electron withdrawing NO_2 substituent. Differences arising from the systematic introduction of 3T–pendants and the NO_2 substituent are illustrated dramatically in the cyclic voltammetry experiments. The potentials for the one electron oxidative processes of the 3T–pendants and the Ir(III)–$(Ph^-{}_{C\wedge N})_2$ moiety are unaffected by each other but the one electron reductive process of the diimine ligand is greatly affected by addition of the NO_2 substituent. These trends are confirmed by DFT calculations that show almost no disturbance in the Ir(III)–$(Ph^-{}_{C\wedge N})_2$ based MO upon addition of 3T–pendants, while considerable stabilization of the diimine based MO is evident upon addition of a NO_2 substituent. Both electrochemical and DFT results suggest that the series should be capable of providing a low lying trap state localized on the NO_2 functionalized diimine ligand.

The excited state properties of the series and the supportive TD-DFT calculations tell a different story. Examination of the absorption spectra of 3T–pendant complexes (**11**

and **12**) shows complete overlap of the bands originating from both the metal and organic chromophores ruling out selective excitation. Aside from control complex **9** and the uncomplexed 3T oligomer **6**, NO_2 functionalized complex **10** is weakly luminescent and no luminescence is observed upon photoexcitation of 3T–pendant complexes at 400 nm in room temperature ACN solutions. TD-DFT calculations suggest that the absence of luminescence from the 3T–pendant complexes results because the lowest excited triplet state is found on the 3T–pendants rather than on the diimine ligand, regardless of the NO_2 substituent.

The systems studied here have merit as potential light-harvesting materials that have been improved through the addition of the strongly absorbing 3T–pendants as secondary chromophores to increase spectral efficacy; however, further tuning of the system energetics will be necessary to direct the excitation energy to a triplet state capable of charge injection. This latter adjustment has proven somewhat difficult to achieve as cationic Ir(III) bis-cyclometalates have higher energy triplet excited states than their Ru(II) polypyridyl counterparts. The use of UV-absorbing pendant chromophores is then required to raise the triplet state energy of the pendant to prevent energy funneling into a noneffective lowest energy state. This strategy is not particularly beneficial for light-harvesting in the visible region, but use of longer wavelength absorbers such as the 3T oligomers used in this study may still provide worth in light-generating devices such as LECs.

Supporting Information: Crystallographic data in CIF format for **10,** additional structural discussion, detailed assignment of TD-DFT transitions, and atom coordinates

for DFT optimized geometries of complexes **9 – 12**. This material is available free of charge via the internet at http://pubs.acs.org.

Corresponding Authors: * E-mail krmann@umn.edu, cramer@umn.edu.

Acknowledgement: The authors would like to thank the University of Minnesota and Victor G. Young of the X–ray crystallographic Facility. Experimental work was funded by a grant from the Chemical Sciences, Geosciences, and Biosciences Division, Office of Basic Energy Sciences, Office of Science, U.S. Department of Energy, under Award DE-FG02-07ER15913. Theoretical work was funded by the National Science Foundation (CHE-0952054).

References

(1) (a) Asbury, J. B.; Ellingson, R. J.; Ghosh, H. N.; Ferrere, S.; Nozik, A. J.; Lian, T. *J. Phys. Chem. B* **1999,** *103*, 3110. (b) Bisquert, J.; Cahen, D.; Hodes, G.; Ruehle, S.; Zaban, A. *J. Phys. Chem. B* **2004,** *108*, 8106. (c) Figgemeier, E.; Hagfeldt, A. *Int. J. Photoenergy* **2004,** *6*, 127. (d) Gao, F.; Wang, Y.; Shi, D.; Zhang, J.; Wang, M.; Jing, X.; Humphry-Baker, R.; Wang, P.; Zakeeruddin, S. M.; Gratzel, M. *J. Am. Chem. Soc.* **2008,** *130*, 10720. (e) Gratzel, M. *J. Photochem. Photobiol.* **2004,** *164*, 3. (f) Hagfeldt, A.; Graetzel, M. *Acc. Chem. Res.* **2000,** *33*, 269. (g) Heimer, T. A.; Heilweil, E. J.; Bignozzi, C. A.; Meyer, G. J. *J. Phys. Chem. A* **2000,** *104*, 4256. (h) Kamat, P. V.; Haria, M.; Hotchandani, S. *J. Phys. Chem. B* **2004,** *108*, 5166. (i) Nazeeruddin, M. K.; De Angelis, F.; Fantacci, S.; Selloni, A.; Viscardi, G.; Liska, P.; Ito, S.; Takeru, B.; Graetzel, M. *J. Am. Chem. Soc.* **2005,** *127*, 16835. (j) Nazeeruddin, M. K.; Zakeeruddin, S. M.; Lagref, J. J.; Liska, P.; Comte, P.; Barolo, C.; Viscardi, G.; Schenk, K.; Graetzel, M. *Coord. Chem. Rev.* **2004,** *248*, 1317. (k) O'Regan, B.; Graetzel, M. *Nature* **1991,** *353*, 737. (l) Yum, J.-H.; Chen, P.; Gratzel, M.; Nazeruddin, M. K. *ChemSusChem* **2008,** *1*, 699.

(2) (a) Lo, K. K.-W.; Chan, J. S.-W.; Lui, L.-H.; Chung, C.-K. *Organometallics* **2004,** *23*, 3108. (b) Lo, K. K.-W.; Hui, W.-K.; Chung, C.-K.; Tsang, K. H.-K.; Lee, T. K.-M.; Li, C.-K.; Lau, J. S.-Y.; Ng, D. C.-M. *Coord. Chem. Rev.* **2006,** *250*, 1724. (c) Lo, K. K.-W.; Tsang, K. H.-K.; Sze, K.-S.; Chung, C.-K.; Lee, T. K.-M.; Zhang, K. Y.; Hui, W.-K.; Li, C.-K.; Lau, J. S.-Y.; Ng, D. C.-M.; Zhu, N. *Coord. Chem. Rev.* **2007,** *251*, 2292. (d) Shao, F.; Elias, B.; Lu, W.; Barton, J. K. *Inorg. Chem.* **2007,** *46*, 10187. (e) Zhang, K. Y.; Lo, K. K.-W. *Inorg. Chem.* **2009,** *48*, 6011.

(3) (a) Borisov, S. M.; Klimant, I. *Anal. Chem.* **2007,** *79*, 7501. (b) Di Marco, G.; Lanza, M.; Mamo, A.; Stefio, I.; Di Pietro, C.; Romeo, G.; Campagna, S. *Anal. Chem.* **1998,** *70*, 5019. (c) Fernandez-Sanchez, J. F.; Roth, T.; Cannas, R.; Nazeeruddin, M. K.; Spichiger, S.; Graetzel, M.; Spichiger-Keller, U. E. *Talanta* **2007,** *71*, 242. (d) Koese, M. E.; Crutchley, R. J.; DeRosa, M. C.; Ananthakrishnan, N.; Reynolds, J. R.; Schanze, K. S. *Langmuir* **2005,** *21*, 8255. (e) Mak, C. S. K.; Pentlehner, D.; Stich, M.; Wolfbeis, O. S.; Chan, W. K.; Yersin, H. *Chem. Mater.* **2009,** *21*, 2173. (f) Marin-Suarezdel Toro, M.; Fernandez-Sanchez, J. F.; Baranoff, E.; Nazeeruddin, M. K.; Graetzel, M.; Fernandez-Gutierrez, A. *Talanta* **2010,** *82*, 620. (g) Xie, Z.; Ma, L.; de Krafft, K. E.; Jin, A.; Lin, W. *J. Am. Chem. Soc.* **2010,** *132*, 922.

(4) (a) Baranoff, E.; Barigelletti, F.; Bonnet, S.; Collin, J.-P.; Flamigni, L.; Mobian, P.; Sauvage, J.-P. *Struct. Bonding* **2007,** *123*, 41. (b) Baranoff, E.; Dixon, I. M.; Collin, J.-P.; Sauvage, J.-P.; Ventura, B.; Flamigni, L. *Inorg. Chem.* **2004,** *43*, 3057. (c) Baranoff, E.; Griffiths, K.; Collin, J.-P.; Sauvage, J.-P.; Ventura, B.; Flamigni, L. *New J. Chem.* **2004,** *28*, 1091. (d) Flamigni, L.; Barbieri, A.; Sabatini, C.; Ventura, B.; Barigelletti, F. *Top. Curr. Chem.* **2007,** *281*, 143. (e) Flamigni, L.; Collin, J.-P.; Sauvage, J.-P. *Acc. Chem. Res.* **2008,** *41*, 857. (f) Flamigni, L.; Ventura, B.; Baranoff, E.; Collin, J.-P.; Sauvage, J.-P. *Eur. J. Inorg. Chem.* **2007**, 5189. (g) Geiss, B.; Lambert, C. *Chem. Commun.* **2009**, 1670. (h) Hanss, D.; Freys, J. C.; Bernardinelli, G.; Wenger, O. S. *Eur. J. Inorg. Chem.* **2009**, 4850.

(5) (a) Cline, E. D.; Adamson, S. E.; Bernhard, S. *Inorg. Chem.* **2008,** *47*, 10378. (b) Fukuzumi, S. *Eur. J. Inorg. Chem.* **2008**, 1351. (c) Fukuzumi, S.; Kobayashi, T.; Suenobu, T. *J. Am. Chem. Soc.* **2010,** *132*, 1496. (d) Goldsmith, J. I.; Hudson, W. R.;

Lowry, M. S.; Anderson, T. H.; Bernhard, S. *J. Am. Chem. Soc.* **2005,** *127*, 7502. (e) Lowry, M. S.; Goldsmith, J. I.; Slinker, J. D.; Rohl, R.; Pascal, R. A., Jr.; Malliaras, G. G.; Bernhard, S. *Chem. Mater.* **2005,** *17*, 5712.

(6) (a) Baranoff, E.; Yum, J.-H.; Graetzel, M.; Nazeeruddin, M. K. *J. Organomet. Chem.* **2009,** *694*, 2661. (b) Baranoff, E.; Yum, J.-H.; Jung, I.; Vulcano, R.; Gratzel, M.; Nazeeruddin, M. K. *Chem. Asian. J.* **2010,** *5*, 496. (c) Huang, J.; Yu, J.; Guan, Z.; Jiang, Y. *Appl. Phys. Lett.* **2010,** *97*, 143301. (d) Mayo, E. I.; Kilsa, K.; Tirrell, T.; Djurovich, P. I.; Tamayo, A.; Thompson, M. E.; Lewis, N. S.; Gray, H. B. *Photochem. Photobiol. Sci.* **2006,** *5*, 871. (e) Ning, Z.; Zhang, Q.; Wu, W.; Tian, H. *J. Organomet. Chem.* **2009,** *694*, 2705.

(7) (a) Bolink, H. J.; Coronado, E.; Garcia Santamaria, S.; Sessolo, M.; Evans, N.; Klein, C.; Baranoff, E.; Kalyanasundaram, K.; Graetzel, M.; Nazeeruddin, M. K. *Chem. Commun.* **2007**, 3276. (b) Bolink, H. J.; De Angelis, F.; Baranoff, E.; Klein, C.; Fantacci, S.; Coronado, E.; Sessolo, M.; Kalyanasundaram, K.; Graetzel, M.; Nazeeruddin, M. K. *Chem. Commun.* **2009**, 4672. (c) Bulovic, V.; Gu, G.; Burrows, P. E.; Forrest, S. R.; Thompson, M. E. *Nature* **1996,** *380*, 29. (d) Chou, P.-T.; Chi, Y. *Chem. Eur. J.* **2007,** *13*, 380. (e) Tamayo, A. B.; Garon, S.; Sajoto, T.; Djurovich, P. I.; Tsyba, I. M.; Bau, R.; Thompson, M. E. *Inorg. Chem.* **2005,** *44*, 8723. (f) Wong, W.-Y.; Ho, C.-L. *Coord. Chem. Rev.* **2009,** *253*, 1709. (g) You, Y.; Park, S. Y. *Dalton Trans.* **2009**, 1267.

(8) (a) Costa, R. D.; Fernández, G.; Sánchez, L.; Martín, N.; Ortí, E.; Bolink, H. J. *Chem. Eur. J.* **2010,** *16*, 9855. (b) Costa, R. D.; Ortí, E.; Bolink, H. J.; Graber, S.; Housecroft, C. E.; Constable, E. C. *Adv. Funct. Mater.* **2010,** *20*, 1511. (c) Costa, R. D.; Ortí, E.; Bolink, H. J.; Graber, S.; Schaffner, S.; Neuburger, M.; Housecroft, C. E.; Constable, E. C. *Adv. Funct. Mater.* **2009,** *19*, 3456. (d) Graber, S.; Doyle, K.; Neuburger, M.; Housecroft, C. E.; Constable, E. C.; Costa, R. D.; Orti, E.; Repetto, D.; Bolink, H. J. *J. Am. Chem. Soc.* **2008,** *130*, 14944. (e) Liu, S.-J.; Zhao, Q.; Fan, Q.-L.; Huang, W. *Eur. J. Inorg. Chem.* **2008,** *2008*, 2177. (f) Rodriguez-Redondo, J. L.; Costa, R. D.; Orti, E.; Sastre-Santos, A.; Bolink, H. J.; Fernandez-Lazaro, F. *Dalton Trans.* **2009**, 9787. (g) Rothe, C.; Chiang, C.-J.; Jankus, V.; Abdullah, K.; Zeng, X.; Jitchati, R.; Batsanov, A. S.; Bryce, M. R.; Monkman, A. P. *Adv. Funct. Mater.* **2009,** *19*, 2038. (h) Shan, G.-G.; Zhu, D.-X.; Li, H.-B.; Li, P.; Su, Z.-M.; Liao, Y. *Dalton Trans.* **2011,** *40*, 2947. (i) Su, H.-C.; Chen, H.-F.; Wu, C.-C.; Wong, K.-T. *Chem. Asian. J.* **2008,** *3*, 1922. (j) Zeng, X.; Tavasli, M.; Perepichka, I. F.; Batsanov, A. S.; Bryce, M. R.; Chiang, C.-J.; Rothe, C.; Monkman, A. P. *Chem. Eur. J.* **2008,** *14*, 933.

(9) (a) Colombo, M. G.; Brunold, T. C.; Riedener, T.; Guedel, H. U.; Fortsch, M.; Buergi, H.-B. *Inorg. Chem.* **1994,** *33*, 545. (b) Colombo, M. G.; Hauser, A.; Guedel, H. U. *Inorg. Chem.* **1993,** *32*, 3088. (c) Dedeian, K.; Djurovich, P. I.; Garces, F. O.; Carlson, G.; Watts, R. J. *Inorg. Chem.* **1991,** *30*, 1685. (d) Dragonetti, C.; Falciola, L.; Mussini, P.; Righetto, S.; Roberto, D.; Ugo, R.; Valore, a. A.; De Angelis, F.; Fantacci, S.; Sgamellotti, A.; Ramon, M.; Muccini, M. *Inorg. Chem.* **2007,** *46*, 8533. (e) Garces, F. O.; King, K. A.; Watts, R. J. *Inorg. Chem.* **1988,** *27*, 3464. (f) Hay, P. J. *J. Phys. Chem. A* **2002,** *106*, 1634. (g) King, K. A.; Spellane, P. J.; Watts, R. J. *J. Am. Chem. Soc.* **1985,** *107*, 1431. (h) Lamansky, S.; Djurovich, P.; Murphy, D.; Abdel-Razzaq, F.; Lee, H. E.; Adachi, C.; Burrows, P. E.; Forrest, S. R.; Thompson, M. E. *J. Am. Chem. Soc.* **2001,** *123*, 4304. (i) Li, X.-N.; Wu, Z.-J.; Zhang, H.-J.; Liu, X.-J.; Zhou, L.; Li, Z.-F.; Si, Z.-J. *Phys. Chem. Chem. Phys.* **2009,** *11*, 6051. (j) Lowry, M. S.; Bernhard, S. *Chem. Eur. J.*

2006, *12*, 7970. (k) Lowry, M. S.; Hudson, W. R.; Pascal, R. A., Jr.; Bernhard, S. *J. Am. Chem. Soc.* **2004,** *126*, 14129. (l) Nazeeruddin, M. K.; Gratzel, M. *Struct. Bonding* **2007,** *123*, 113. (m) Nazeeruddin, M. K.; Humphry-Baker, R.; Berner, D.; Rivier, S.; Zuppiroli, L.; Graetzel, M. *J. Am. Chem. Soc.* **2003,** *125*, 8790. (n) Ohsawa, Y.; Sprouse, S.; King, K. A.; DeArmond, M. K.; Hanck, K. W.; Watts, R. J. *J. Phys. Chem.* **1987,** *91*, 1047. (o) Tamayo, A. B.; Alleyne, B. D.; Djurovich, P. I.; Lamansky, S.; Tsyba, I.; Ho, N. N.; Bau, R.; Thompson, M. E. *J. Am. Chem. Soc.* **2003,** *125*, 7377. (p) Waern, J. B.; Desmarets, C.; Chamoreau, L.-M.; Amouri, H.; Barbieri, A.; Sabatini, C.; Ventura, B.; Barigelletti, F. *Inorg. Chem.* **2008,** *47*, 3340.

(10) (a) Bandini, M.; Bianchi, M.; Valenti, G.; Piccinelli, F.; Paolucci, F.; Monari, M.; Umani-Ronchi, A.; Marcaccio, M. *Inorg. Chem.* **2010,** *49*, 1439. (b) King, K. A.; Watts, R. J. *J. Am. Chem. Soc.* **1987,** *109*, 1589. (c) Ladouceur, S. b.; Fortin, D.; Zysman-Colman, E. *Inorg. Chem.* **2010,** *49*, 5625.

(11) (a) Baldo, M. A.; Lamansky, S.; Burrows, P. E.; Thompson, M. E.; Forrest, S. R. *Appl. Phys. Lett.* **1999,** *75*, 4. (b) Baldo, M. A.; O'Brien, D. F.; You, Y.; Shoustikov, A.; Sibley, S.; Thompson, M. E.; Forrest, S. R. *Nature* **1998,** *395*, 151. (c) Chen, X.; Liao, J.-L.; Liang, Y.; Ahmed, M. O.; Tseng, H.-E.; Chen, S.-A. *J. Am. Chem. Soc.* **2003,** *125*, 636. (d) D'Andrade, B. W.; Baldo, M. A.; Adachi, C.; Brooks, J.; Thompson, M. E.; Forrest, S. R. *Appl. Phys. Lett.* **2001,** *79*, 1045. (e) Sandee, A. J.; Williams, C. K.; Evans, N. R.; Davies, J. E.; Boothby, C. E.; Köhler, A.; Friend, R. H.; Holmes, A. B. *J. Am. Chem. Soc.* **2004,** *126*, 7041. (f) Schulz, G. L.; Chen, X.; Chen, S.-A.; Holdcroft, S. *Macromolecules* **2006,** *39*, 9157. (g) Wang, L.; Lei, G.; Qiu, Y. *J. Appl. Phys.* **2005,** *97*, 114503. (h) Yan, Q.; Yue, K.; Yu, C.; Zhao, D. *Macromolecules* **2010,** *43*, 8479.

(12) (a) Ding, J.; Lü, J.; Cheng, Y.; Xie, Z.; Wang, L.; Jing, X.; Wang, F. *Adv. Funct. Mater.* **2008,** *18*, 2754. (b) Qin, T.; Ding, J.; Wang, L.; Baumgarten, M.; Zhou, G.; Müllen, K. *J. Am. Chem. Soc.* **2009,** *131*, 14329.

(13) (a) Bair, J. S.; Harrison, R. G. *J. Org. Chem.* **2007,** *72*, 6653. (b) Barbieri, A.; Ventura, B.; Flamigni, L.; Barigelletti, F.; Fuhrmann, G.; Bäuerle, P.; Goeb, S.; Ziessel, R. *Inorg. Chem.* **2005,** *44*, 8033. (c) Hjelm, J.; Handel, R. W.; Hagfeldt, A.; Constable, E. C.; Housecroft, C. E.; Forster, R. J. *Inorg. Chem.* **2005,** *44*, 1073. (d) Moorlag, C.; Wolf, M. O. *Polym. Prepr.* **2007,** *48*, 543. (e) Pappenfus, T. M.; Mann, K. R. *Inorg. Chem.* **2001,** *40*, 6301. (f) Sauvage, F.; Fischer, M. K. R.; Mishra, A.; Zakeeruddin, S. M.; Nazeeruddin, M. K.; Baeuerle, P.; Graetzel, M. *ChemSusChem* **2009,** *2*, 761. (g) Steen, R. O.; Nurkkala, L. J.; Angus-Dunne, S. J.; Schmitt, C. X.; Constable, E. C.; Riley, M. J.; Bernhardt, P. V.; Dunne, S. J. *Eur. J. Inorg. Chem.* **2008,** *2008*, 1784. (h) Stott, T. L.; Wolf, M. O. *Coord. Chem. Rev.* **2003,** *246*, 89. (i) Yin, J.-F.; Chen, J.-G.; Lu, Z.-Z.; Ho, K.-C.; Lin, H.-C.; Lu, K.-L. *Chem. Mater.* **2010,** *22*, 4392. (j) Ziessel, R.; Bauerle, P.; Ammann, M.; Barbieri, A.; Barigelletti, F. *Chem. Commun.* **2005**, 802.

(14) (a) Beek, W. J. E.; Janssen, R. A. J. *Adv. Funct. Mater.* **2002,** *12*, 519. (b) Casado, J.; Pappenfus, T. M.; Miller, L. L.; Mann, K. R.; Orti, E.; Viruela, P. M.; Pou-Amerigo, R.; Hernandez, V.; Lopez Navarrete, J. T. *J. Am. Chem. Soc.* **2003,** *125*, 2524. (c) Facchetti, A.; Yoon, M.-H.; Stern, C. L.; Hutchison, G. R.; Ratner, M. A.; Marks, T. J. *J. Am. Chem. Soc.* **2004,** *126*, 13480. (d) Huss, A. S.; Pappenfus, T.; Bohnsack, J.; Burand, M.; Mann, K. R.; Blank, D. A. *J. Phys. Chem. A* **2009,** *113*, 10202. (e) Pappenfus, T. M.; Burand, M. W.; Janzen, D. E.; Mann, K. R. *Org. Lett.* **2003,** *5*, 1535. (f) Roncali, J. *Acc. Chem. Res.* **2009,** *42*, 1719. (g) Tian, H.; Shi, J.; He, B.; Hu, N.;

Dong, S.; Yan, D.; Zhang, J.; Geng, Y.; Wang, F. *Adv. Funct. Mater.* **2007,** *17*, 1940. (h) Won, Y. S.; Yang, Y. S.; Kim, J. H.; Ryu, J.-H.; Kim, K. K.; Park, S. S. *Energy Fuels* **2010,** *24*, 3676. (i) Xia, P. F.; Feng, X. J.; Lu, J.; Tsang, S.-W.; Movileanu, R.; Tao, Y.; Wong, M. S. *Adv. Mater.* **2008,** *20*, 4810.

(15) Araya, J. C.; Gajardo, J.; Moya, S. A.; Aguirre, P.; Toupet, L.; Williams, J. A. G.; Escadeillas, M.; Le Bozec, H.; Guerchais, V. *New J. Chem* **2010,** *34*, 21.

(16) (a) Bolink, H. J.; Coronado, E.; Costa, R. D.; Lardies, N.; Orti, E. *Inorg. Chem.* **2008,** *47*, 9149. (b) He, L.; Duan, L.; Qiao, J.; Wang, R.; Wei, P.; Wang, L.; Qiu, Y. *Adv. Funct. Mater.* **2008,** *18*, 2123. (c) Zhao, Q.; Liu, S.; Shi, M.; Wang, C.; Yu, M.; Li, L.; Li, F.; Yi, T.; Huang, C. *Inorg. Chem.* **2006,** *45*, 6152.

(17) Demnitz, F. W. J.; D'heni, M. B. *Org. Prep. Proced. Int.* **1998,** *30*, 467

(18) Zhu, S. S.; Kingsborough, R. P.; Swager, T. M. *J. Mater. Chem.* **1999,** *9*, 2123.

(19) Wang, C.; Benz, M. E.; LeGoff, E.; Schindler, J. L.; Allbritton-Thomas, J.; Kannewurf, C. R.; Kanatzidis, M. G. *Chem. Mater.* **1994,** *6*, 401.

(20) Sprouse, S.; King, K. A.; Spellane, P. J.; Watts, R. J. *J. Am. Chem. Soc.* **1984,** *106*, 6647.

(21) Wenkert, D.; Woodward, R. B. *J. Org. Chem.* **1983,** *48*, 283.

(22) Comins, D. L.; Mantlo, N. B. *J. Org. Chem.* **1985,** *50*, 4410.

(23) Araki, K.; Endo, H.; Masuda, G.; Ogawa, T. *Chem. Eur. J.* **2004,** *10*, 3331.

(24) (a) Graf, D. D.; Mann, K. R. *Inorg. Chem.* **1997,** *36*, 150. (b) Graf, D. D.; Mann, K. R. *Inorg. Chem.* **1997,** *36*, 141.

(25) (a) Blessing, R. H. *Acta Crystallogr., Sect. A* **1995,** *51*, 33. (b) Sheldrick, G. *SADABS*, v.2.03; Bruker AXS: Madison, WI, 2002.

(26) *SHELXTL*, v.6.1; Bruker AXS: Madison, WI, 2001.

(27) Zhao, Y.; Truhlar, D. G. *J. Chem. Phys.* **2006,** *125*, 194101.

(28) Hehre, W. J.; Radom, L.; Schleyer, P. v. R.; Pople, J. A. *Ab Initio Molecular Orbital Theory;* John Wiley & Sons: New York, 1986.

(29) Andrae, D.; Häußermann, U.; Dolg, M.; Stoll, H.; Preuß, H. *Theoretica Chimica Acta* **1990,** *77*, 123.

(30) Frisch, M. J.; Trucks, G. W.; Shchlegel, H. B.; Scuseria, G. E.; Robb, M. A.; Cheeseman, J. R.; Scalmani, G.; Barone, V.; Mennucci, B.; Petersson, G. A.; Nakatsuji, H.; Caricato, M.; Li, X.; Hratchian, H. P.; Izmaylov, A. F.; Bloino, J.; Zheng, G.; Sonnenberg, J. L.; Hada, M.; Ehara, M.; Toyota, K.; Fukuda, R.; Hasegawa, J.; Ishida, M.; Nakajima, T.; Honda, Y.; Kitao, O.; Nakai, H.; Vreven, T.; Montgomery, J., J. A.; Peralta, J. E.; Ogliaro, F.; Bearpark, M.; Heyd, J. J.; Brothers, E.; Kudin, K. N.; Staroverov, V. N.; Kobayashi, R.; Normand, J.; Raghavachari, K.; Rendell, A.; Burant, J. C.; Iyengar, S. S.; Tomasi, J.; Cossi, M.; Rega, N.; Millam, N. J.; Klene, M.; Knox, J. E.; Cross, J. B.; Bakken, V.; Adamo, C.; Jaramillo, J.; Gomperts, R.; Stratmann, R. E.; Yazyev, O.; Austin, A. J.; Cammi, R.; Pomelli, C.; Ochterski, J. W.; Martin, R. L.; Morokuma, K.; Zakrzewski, V. G.; Voth, G. A.; Salvador, P.; Dannenberg, J. J.; Dapprich, S.; Daniels, A. D.; Farkas, Ö.; Foresman, J. B.; Ortiz, J. V.; Cioslowski, J.; Fox, D. J. *Gaussian 09*, Gaussian, Inc.: Wallingford, CT, 2009.

(31) Cramer, C. J. *Essentials of Computational Chemistry: Theories and Models;* Second ed.; John Wiley & Sons, Ltd: Chichester, U.K., 2004.

(32) Marenich, A. V.; Cramer, C. J.; Truhlar, D. G. *J. Phys. Chem. B* **2009,** *113*, 6378.

(33) (a) Runge, E.; Gross, E. K. U. *Phys. Rev. Lett.* **1984,** *52*, 997. (b) Cammi, R.; Mennucci, B.; Tomasi, J. *J. Phys. Chem. A* **2000,** *104*, 5631.

(34) Zhao, Y.; Truhlar, D. G. *Acc. Chem. Res.* **2008,** *41*, 157.

(35) (a) Jiang, W.; Gao, Y.; Sun, Y.; Ding, F.; Xu, Y.; Bian, Z.; Li, F.; Bian, J.; Huang, C. *Inorg. Chem.* **2010,** *49*, 3252. (b) Zhao, Q.; Liu, S.; Shi, M.; Li, F.; Jing, H.; Yi, T.; Huang, C. *Organometallics* **2007,** *26*, 5922.

(36) Allen, F. H. *Acta Crystallogr., Sect. B* **2002,** *B58*, 380.

(37) (a) Chen, C.-T.; Lin, T.-Y. J.; Chen, C.-H.; Lin, K.-J. *J. Chin. Chem. Soc.* **2000,** *47*, 197. (b) Kinnunen, T.-J. J.; Haukka, M.; Nousiainen, M.; Patrikka, A.; Pakkanen, T. A. *J. Chem. Soc., Dalton Trans.* **2001**, 2649.

(38) (a) Busby, M.; Gabrielsson, A.; Matousek, P.; Towrie, M.; Di Bilio, A. J.; Gray, H. B.; Vlček, A. *Inorg. Chem.* **2004,** *43*, 4994. (b) Bush, P. M.; Whitehead, J. P.; Pink, C. C.; Gramm, E. C.; Eglin, J. L.; Watton, S. P.; Pence, L. E. *Inorg. Chem.* **2001,** *40*, 1871. (c) Chen, X.-F.; Cheng, P.; Liu, X.; Zhao, B.; Liao, D.-Z.; Yan, S.-P.; Jiang, Z.-H. *Inorg. Chem.* **2001,** *40*, 2652. (d) Lam, S. C.-F.; Yam, V. W.-W.; Wong, K. M.-C.; Cheng, E. C.-C.; Zhu, N. *Organometallics* **2005,** *24*, 4298.

(39) (a) Basu, A.; Weiner, M. A.; Strekas, T. C.; Gafney, H. D. *Inorg. Chem.* **1982,** *21*, 1085. (b) Canivet, J.; Süss-Fink, G.; Štěpnička, P. *Eur. J. Inorg. Chem.* **2007,** *2007*, 4736. (c) Morotti, T.; Pizzotti, M.; Ugo, R.; Quici, S.; Bruschi, M.; Mussini, P.; Righetto, S. *Eur. J. Inorg. Chem.* **2006,** *2006*, 1743. (d) Stepnicka, P.; Ludvík, J.; Canivet, J.; Süss-Fink, G. *Inorg. Chim. Acta* **2006,** *359*, 2369.

(40) Murray, P.; Jack, L.; McInnes, E. J. L.; Yellowlees, L. J. *Dalton Trans.* **2010,** *39*, 4179.

(41) (a) Colombo, M.; Hauser, A.; Güdel, H. *Top. Curr. Chem.* **1994,** *171*, 143. (b) Colombo, M. G.; Guedel, H. U. *Inorg. Chem.* **1993,** *32*, 3081. (c) Dixon, I. M.; Collin, J.-P.; Sauvage, J.-P.; Flamigni, L.; Encinas, S.; Barigelletti, F. *Chem. Soc. Rev.* **2000,** *29*, 385. (d) Lafolet, F.; Welter, S.; Popovic, Z.; Cola, L. D. *J. Mater. Chem.* **2005,** *15*, 2820. (e) Wilde, A. P.; King, K. A.; Watts, R. J. *J. Phys. Chem.* **1991,** *95*, 629.

(42) (a) Rubio, M.; Merchán, M.; Ortí, E. *ChemPhysChem* **2005,** *6*, 1357. (b) Wasserberg, D.; Marsal, P.; Meskers, S. C. J.; Janssen, R. A. J.; Beljonne, D. *J. Phys. Chem. B* **2005,** *109*, 4410.

(43) (a) Hissler, M.; Connick, W. B.; Geiger, D. K.; McGarrah, J. E.; Lipa, D.; Lachicotte, R. J.; Eisenberg, R. *Inorg. Chem.* **2000,** *39*, 447. (b) Villegas, J. M.; Stoyanov, S. R.; Huang, W.; Rillema, D. P. *Inorg. Chem.* **2005,** *44*, 2297.

(44) (a) Crespo-Hernández, C. E.; Burdzinski, G.; Arce, R. *J. Phys. Chem. A* **2008,** *112*, 6313. (b) Farztdinov, V. M.; Schanz, R.; Kovalenko, S. A.; Ernsting, N. P. *J. Phys. Chem. A* **2000,** *104*, 11486. (c) Kovalenko, S. A.; Schanz, R.; Farztdinov, V. M.; Hennig, H.; Ernsting, N. P. *Chem. Phys. Lett.* **2000,** *323*, 312. (d) Mohammed, O. F.; Vauthey, E. *J. Phys. Chem. A* **2008,** *112*, 3823. (e) Takezaki, M.; Hirota, N.; Terazima, M.; Sato, H.; Nakajima, T.; Kato, S. *J. Phys. Chem. A* **1997,** *101*, 5190.

(45) Laye, R. H.; Couchman, S. M.; Ward, M. D. *Inorg. Chem.* **2001,** *40*, 4089.

(46) (a) Kozhevnikov, D. N.; Kozhevnikov, V. N.; Shafikov, M. Z.; Prokhorov, A. M.; Bruce, D. W.; Gareth Williams, J. A. *Inorg. Chem.* **2011,** *50*, 3804. (b) Spaenig, F.; Olivier, J.-H.; Prusakova, V.; Retailleau, P.; Ziessel, R.; Castellano, F. N. *Inorg. Chem.* **2011,** *50*, 10859.

TOC Artwork and Synopsis

Photoexcitation (λ_{ex} = 400 nm) of the pictured thiophene oligomer (H3T-ppy) and $[Ir(ppy)_2(bpy)]PF_6$ provide strong luminescence. In stark contrast hybrid metal-organic complex $[Ir(3T\text{-}ppy)(bpy)]PF_6$ bears terthiophene (3T) pendants, ligated through the cyclometalating ppy cap, displays near total quenching of luminescence at the same excitation wavelength. As indicated by DFT / TD-DFT calculations, the state diagram depicted below shows the lowest energy excited state is located on the 3T–pendant, rationalizing the absence of luminescence.